

- Supplementary Information -

**Probing Substrate Binding and Release Events
in Iridium-Catalysed Hydrogen Isotope Exchange Reactions**

Daria S. Timofeeva, William J. Kerr,* David M. Lindsay,* and David J. Nelson*

Department of Pure and Applied Chemistry, University of Strathclyde,
295 Cathedral Street, Glasgow, G1 1XL, UK

david.lindsay@strath.ac.uk, w.kerr@strath.ac.uk, david.nelson@strath.ac.uk

Table of Contents

1.	General experimental details	S2
2.	Synthesis and characterisation of compounds	S3
3.	Kinetic data	
3.1	General kinetic protocol for reaction monitoring by sampling	S12
3.2	Mass spectrometry analysis for isotopologue distribution over time	S13
3.3	Kinetic data/isotopologue distribution for substituted phenylpyridines	S22
3.4	Hammett plot for substituted phenylpyridines	S37
4.	Computational chemistry	
4.1	General computational details	S38
4.2	Energies of optimised structures	S39
4.3	Energy decomposition analysis	S41
4.4	IRC electronic energy plots	S42
4.5	Coordinates of optimised structures	S42
5.	Literature data on Lewis basicity	S43
6.	References	S44

1. General experimental details

General

For the synthetic procedures, standard Schlenk techniques using an inert gas atmosphere (argon or nitrogen) were used, unless otherwise stated. Materials obtained from commercial sources (acetophenone, ethyl benzoate, nitrobenzene, 2-phenylpyridine, 1-phenylpyrazole, 2-phenyloxazoline) were used without further purification. All glassware was flame dried and cooled under a stream of nitrogen or argon prior to use.

Materials

(1,3-bis-(2,4,6-trimethylphenyl)imidazolium chloride,¹ 2-phenylpyrimidine,² 1-methyl-2-phenylimidazole³ and 4-substituted 2-phenylpyridines⁴ were synthesised according to literature procedures. Anhydrous Na[BAr^F₂₄] (BAr^F₂₄ = tetrakis[3,5-bis(trifluoromethyl)phenyl]borate)) was obtained following Bergman's synthesis,⁵ followed by recrystallising the crude Na[BArF₂₄]^x(solvent) prior to drying.⁶ [Ir(COD)(IMes)(PPh₃)][BAr^F₂₄] was synthesised from [IrCl(COD)(IMes)]⁷ in a procedure adapted from that published before for the preparation of the corresponding complexes with BF₄ and OTf counterions.⁸

Flash column chromatography was carried out using silica gel (230-400 mesh). Thin layer chromatography (TLC) was performed using Merck silica plates coated with fluorescent indicator and visualised by UV light (254 nm).

Analysis

¹H (400 MHz) and ¹³C{¹H} (101 MHz) NMR spectra were obtained on a Bruker AV3-400 instrument with a liquid nitrogen Prodigy cryoprobe. The chemical shifts (δ) are reported in ppm relative to the residual protonated solvent for ¹H NMR or the solvent signal for ¹³C{¹H} NMR (CDCl₃: δ_{H} 7.26 ppm and δ_{C} 77.16 ppm).⁵⁹ Multiplicities are expressed as s (singlet), d (doublet), t (triplet), q (quartet), m (multiplet), or br (broad signal). If no multiplicity is given for ¹³C{¹H} NMR data, the signal is a singlet. NMR assignments were made using additional 2D NMR experiments where necessary.

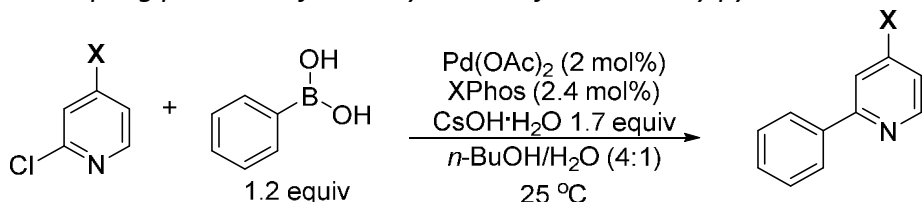
LC-MS analyses were carried out using Agilent 6130 with 1200 series LC and UV at 254 nm, with Agilent Poroshell 120 LC column (EC C18 2.7 μ m x 4.6mm x75mm). LC column conditions were as follows: mobile phase A: water + 5mM ammonium acetate; mobile phase B: acetonitrile + 5mM ammonium acetate; Flow rate: 1.000 mL/min.

Timetable:	Time, min	0	1.48	8.50	13.5	16.5	18.0
	%A	95	95	100	100	95	95
	%B	5	5	0	0	5	5

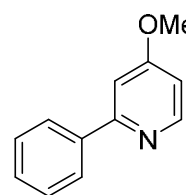
GC-MS analyses were carried out using an Agilent 7890A gas chromatograph fitted with a ZB-5 MS column (30 m x 0.25 mm I.D. x 0.25 μ m) and an Agilent 5975C MSD running in EI mode.

2. Synthesis and characterisation

General cross-coupling procedure for the synthesis of 4-X-2-Phenylpyridines⁴



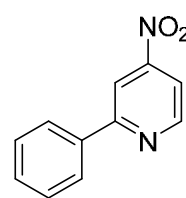
Under argon or nitro-gen, a 100 mL Schlenk flask containing a magnetic stirrer bar was sequentially charged with $\text{Pd}(\text{OAc})_2$ (16 mg, 0.07 mmol), XPhos (39 mg, 0.08 mmol), 4-X-2-chloropyridine (4 mmol), phenylboronic acid (509 mg, 4.18 mmol), and degassed *n*-butanol (12 mL). The mixture was stirred at 25 °C for 15 min, and then a solution of $\text{CsOH}\cdot\text{H}_2\text{O}$ (887 mg, 5.92 mmol) in degassed H_2O (3 mL) was added in one portion to initiate the Suzuki-Miyaura reaction. The reaction mixture was stirred vigorously at 25 °C until all the heteroaryl chloride was consumed (monitored by GC or TLC). At the end of the reaction, the organic phase was separated, and the aqueous phase was further extracted with ethyl acetate (20 mL x 3). The organic extracts were combined and concentrated on a rotary evaporator. The resulting residue was purified by silica gel flash chromatography to provide the desired coupling product.

 **4-methoxy-2-phenylpyridine** was synthesized according general cross-coupling procedure using 2-chloro-4-methoxypyridine (500 mg, 3.48 mmol). After flash chromatography with ethyl acetate/hexane (1:8) as eluent, the title compound was isolated as a colourless oil (482 mg, 74% yield).

$^1\text{H NMR}$ (400 MHz, CDCl_3) δ 8.52 (d, $J = 5.7$ Hz, 1H), 7.98 – 7.94 (m, 2H), 7.50 – 7.38 (m, 3H), 7.23 (d, $J = 2.4$ Hz, 1H), 6.77 (dd, $J = 5.7, 2.4$ Hz, 1H), 3.90 (s, 3H).

$^{13}\text{C}\{^1\text{H}\} \text{ NMR}$ (101 MHz, CDCl_3) δ 166.5, 159.4, 151.0, 139.6, 129.1, 128.8, 127.1, 108.2, 107.0, 55.3.

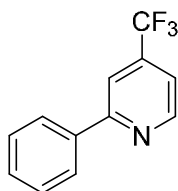
NMR data are consistent with the literature.⁹

 **4-nitro-2-phenylpyridine** was synthesized according general cross-coupling procedure using 2-chloro-4-nitropyridine (552 mg, 3.48 mmol). After solvent evaporation, the title compound crystallised overnight, filtered and washed with pentane isolated as beige solid (340 mg, 49% yield).

$^1\text{H NMR}$ (400 MHz, CDCl_3) δ 8.97 (d, $J = 5.6$ Hz, 1H), 8.45 (d, $J = 1.6$ Hz, 1H), 8.12 – 8.06 (m, 2H), 7.94 (dd, $J = 5.3, 2.0$ Hz, 1H), 7.59 – 7.48 (m, 3H).

$^{13}\text{C}\{^1\text{H}\} \text{ NMR}$ (101 MHz, CDCl_3) δ 160.6, 155.0, 151.9, 137.4, 130.6, 129.3, 127.3, 114.4, 112.9.

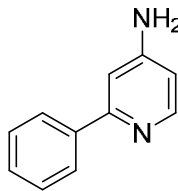
NMR data are consistent with the literature.¹⁰



4-trifluoromethyl-2-phenylpyridine was synthesized according general cross-coupling procedure using 2-chloro-4-trifluoromethyl pyridine (632 mg, 3.48 mmol). After flash chromatography with ethyl acetate/hexane (1:10) as eluent, the title compound was isolated as a colourless oil (605 mg, 78% yield).

¹H NMR (400 MHz, CDCl₃) δ 8.87 (d, *J* = 5.1 Hz, 1H), 8.07 – 7.99 (m, 2H), 7.95 – 7.91 (m, 1H), 7.55 – 7.42 (m, 4H). **¹³C{¹H} NMR** (101 MHz, CDCl₃) δ 159.0, 150.8, 139.3 (q, ²J_{C-F} = 34.1 Hz), 138.2, 130.0, 129.1, 127.2, 123.1 (q, ¹J_{C-F} = 269.8 Hz), 117.7 (q, ³J_{C-F} = 3.4 Hz), 116.2 (q, ³J_{C-F} = 3.3 Hz). **¹⁹F NMR** (376 MHz, CDCl₃) δ -64.83 (s).

NMR data are consistent with the literature.¹¹



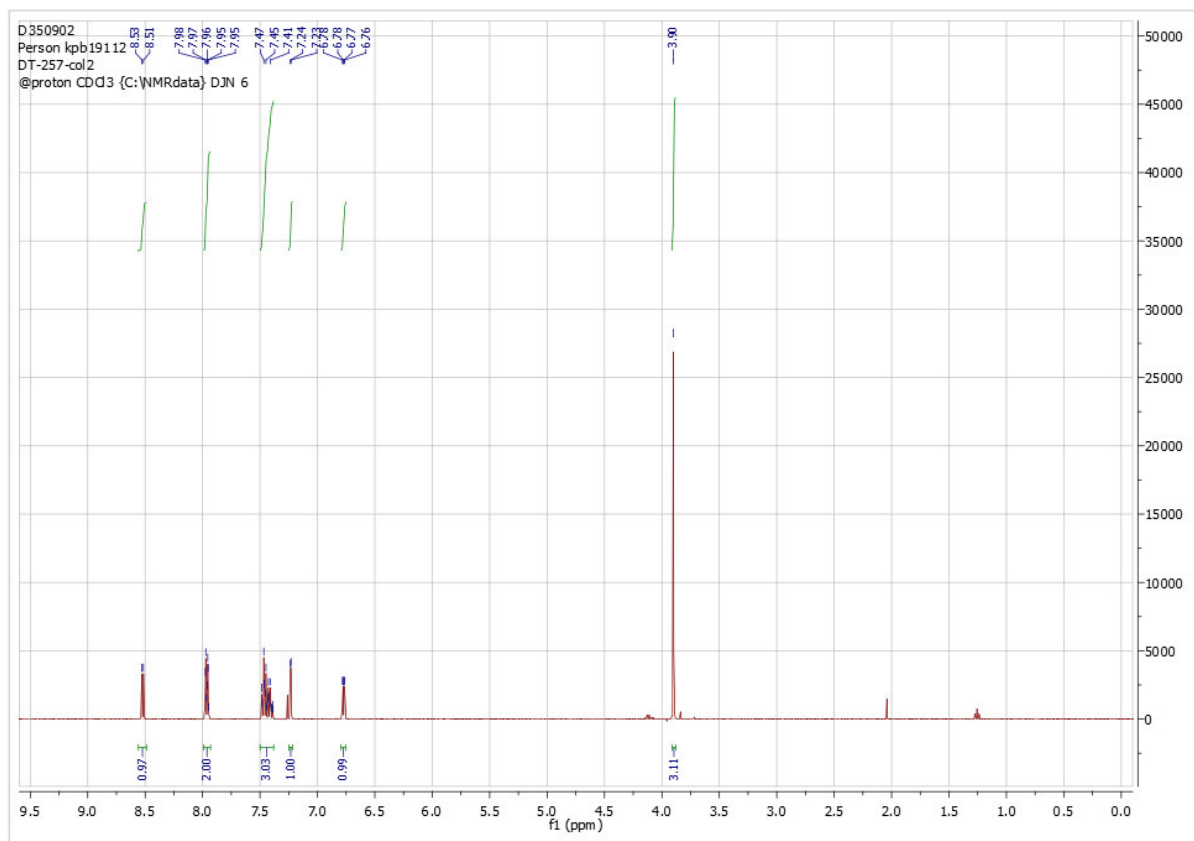
4-amino-2-phenylpyridine was synthesized according general cross-coupling procedure using 2-chloro-4-aminopyridine (632 mg, 3.48 mmol). After flash chromatography starting with ethyl acetate/hexane (1:4) as eluent followed by ethyl acetate/hexane (1:2) and ethyl acetate/MeOH (10:1) mixture, the title compound was isolated as yellow solid (180 mg, 30% yield).

¹H NMR (400 MHz, CDCl₃) δ 8.26 (d, *J* = 5.6 Hz, 1H), 7.86 (m, 2H), 7.45 – 7.37 (m, 3H), 6.91 (d, *J* = 2.1 Hz, 1H), 6.46 (dd, *J* = 5.6, 2.2 Hz, 1H), 4.33 (br. s, 2H). **¹³C{¹H} NMR** (101 MHz, CDCl₃) δ 158.2, 153.8, 149.7, 139.5, 129.0, 128.7, , 127.1, 108.5, 106.7.

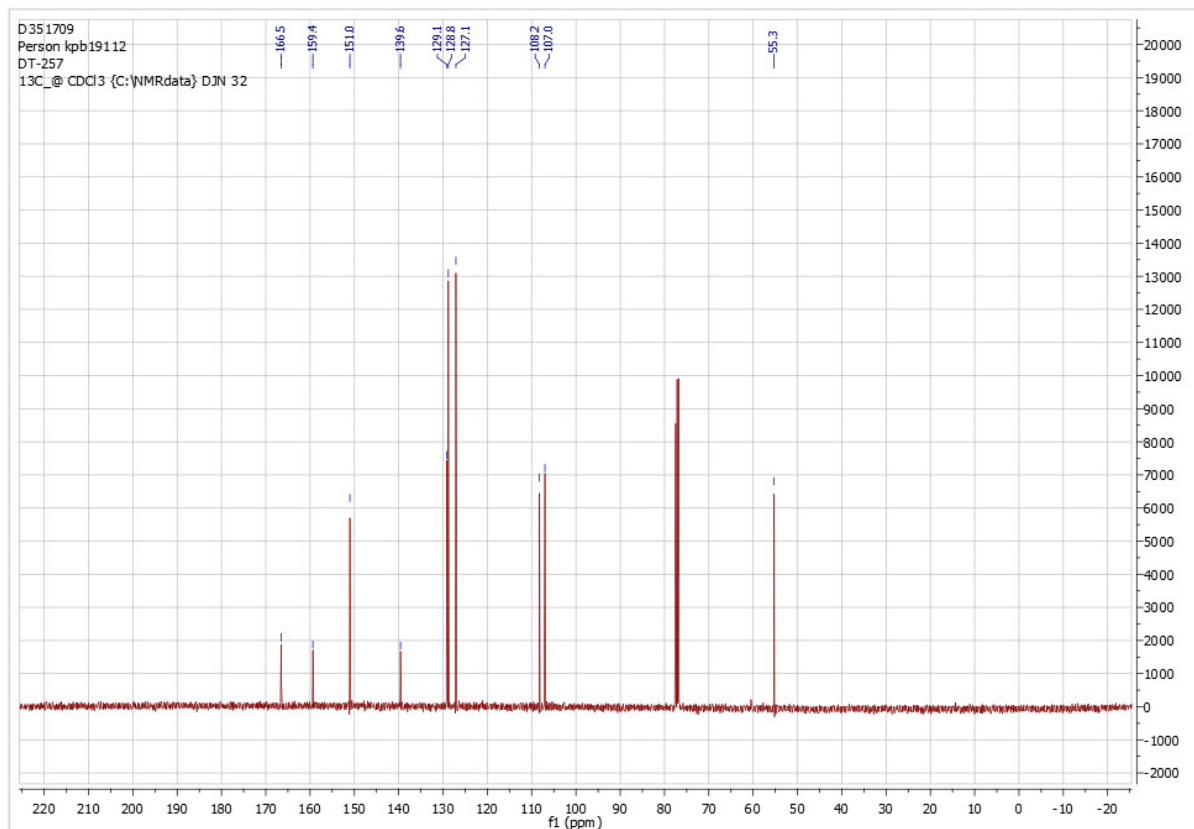
NMR data are consistent with the literature.¹²

NMR spectra for substituted 2-phenylpyridine substrates

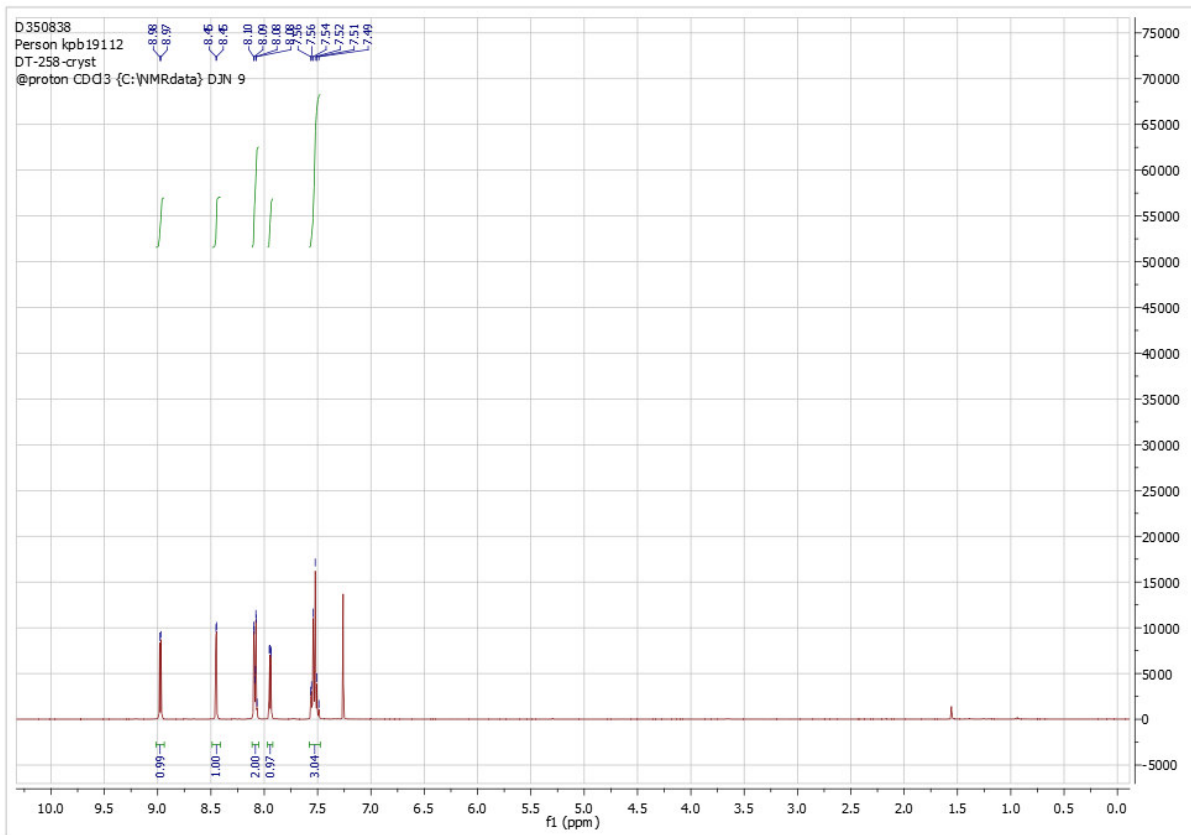
4-methoxy-2-phenylpyridine: ^1H



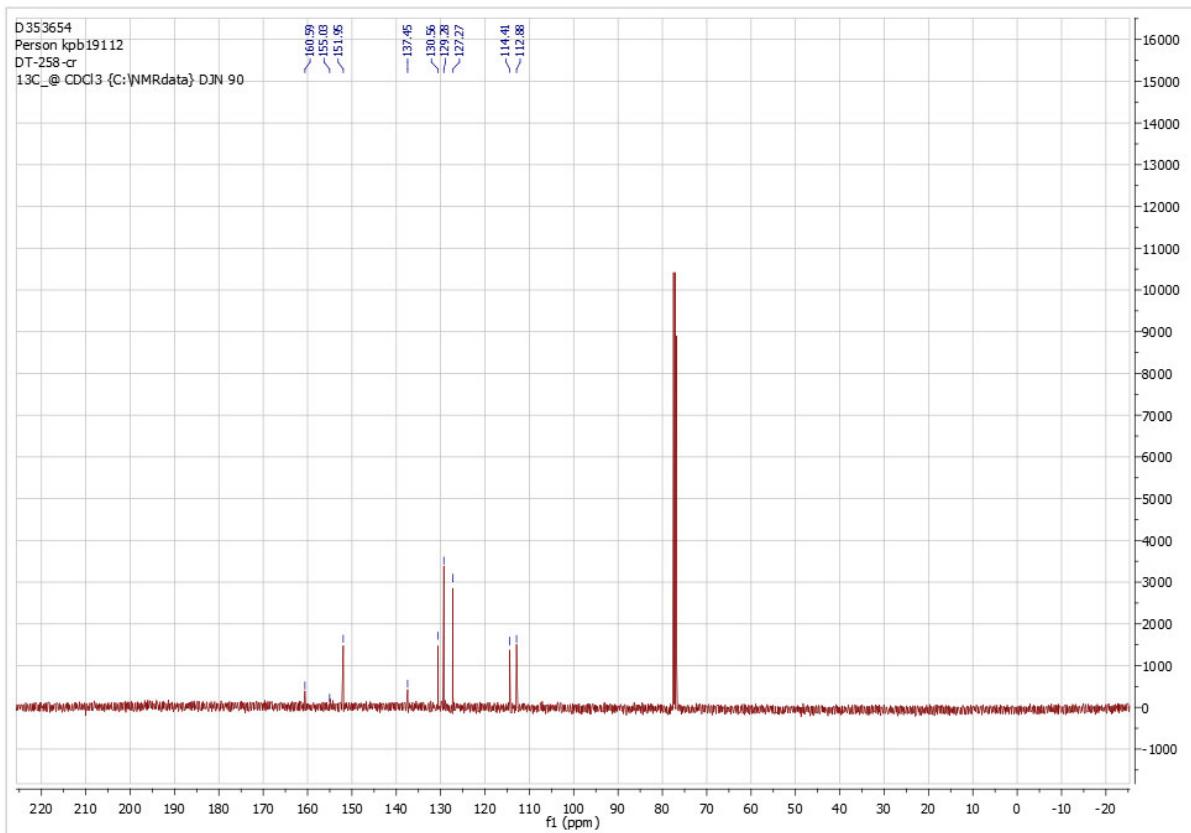
4-methoxy-2-phenylpyridine: $^{13}\text{C}\{^1\text{H}\}$



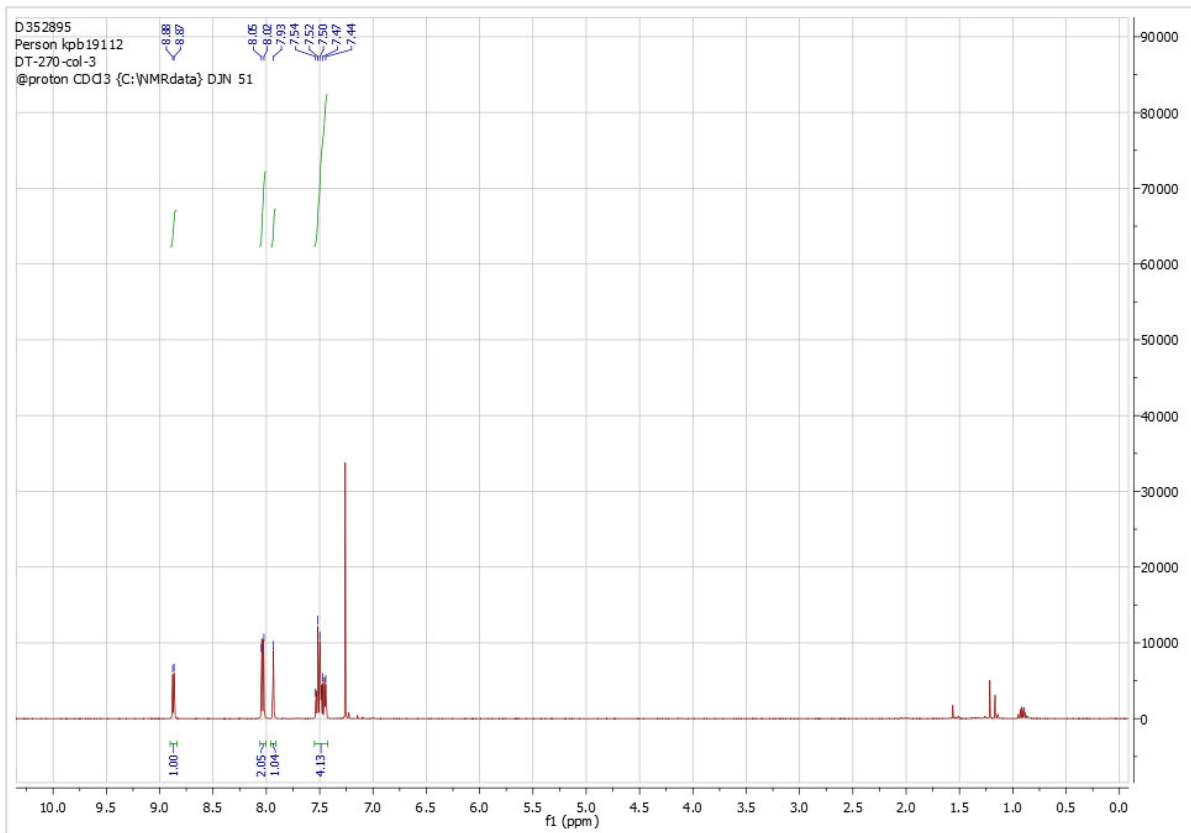
4-nitro-2-phenylpyridine: ^1H



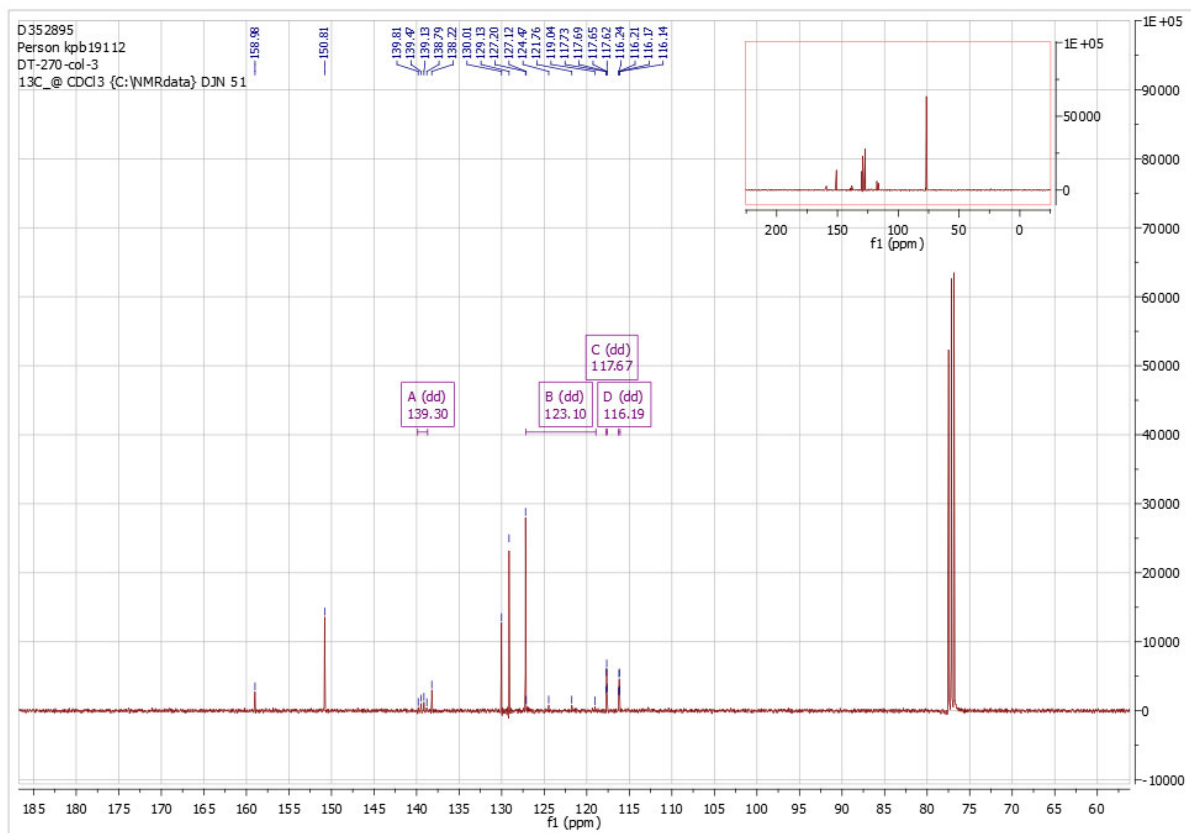
4-nitro-2-phenylpyridine: $^{13}\text{C}\{^1\text{H}\}$



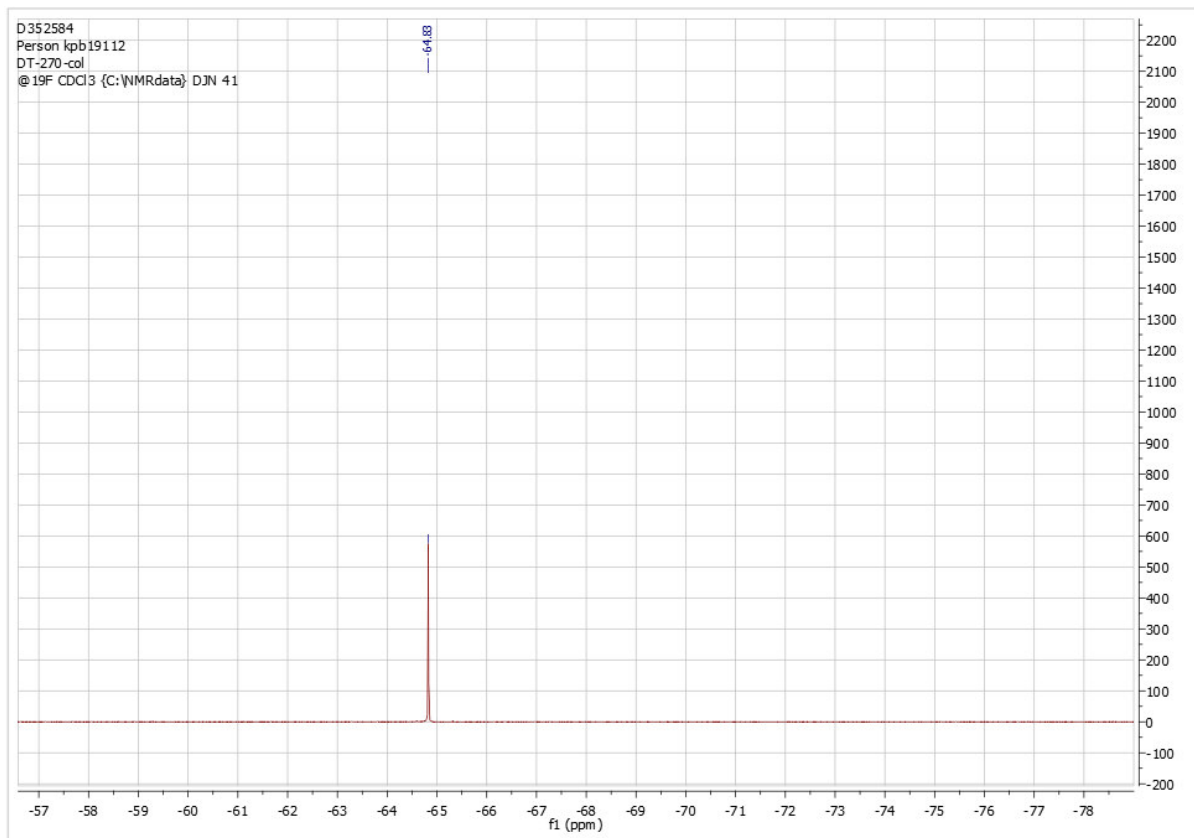
4-trifluoromethyl-2-phenylpyridine: ^1H



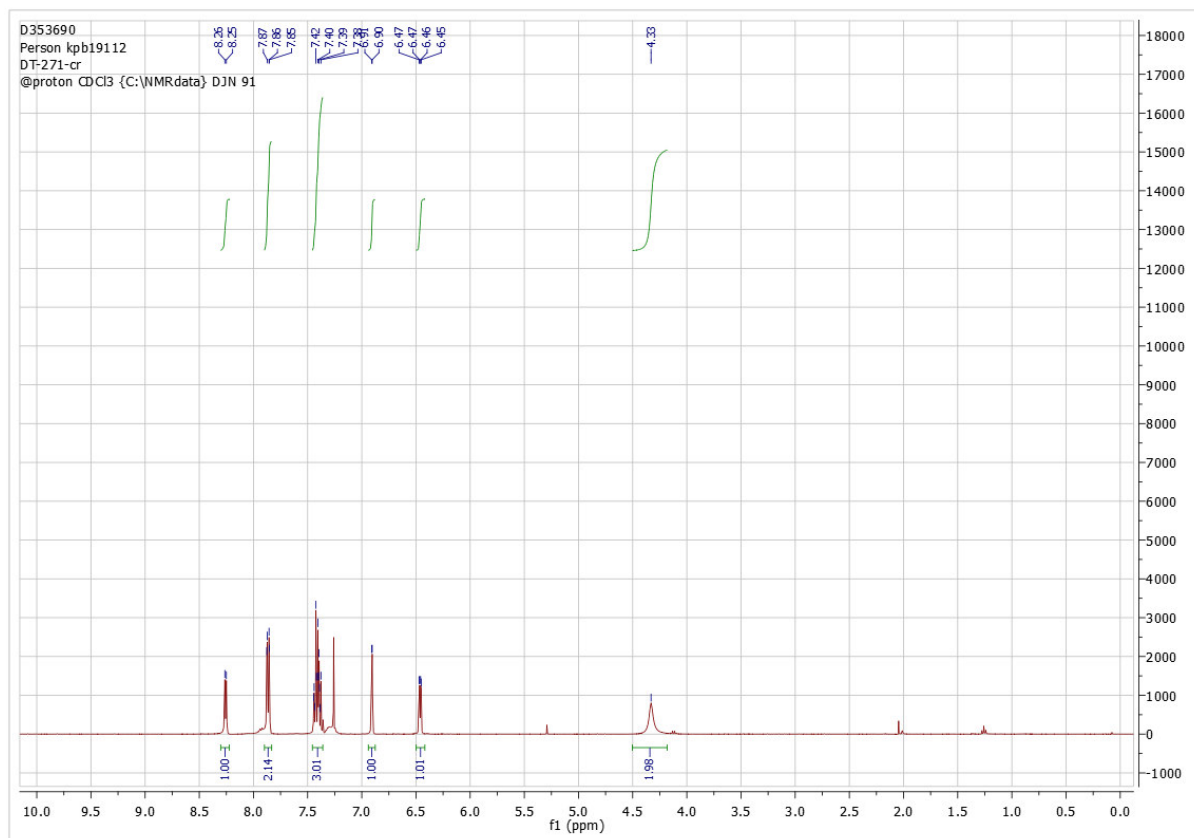
4-trifluoromethyl-2-phenylpyridine: $^{13}\text{C}\{^1\text{H}\}$



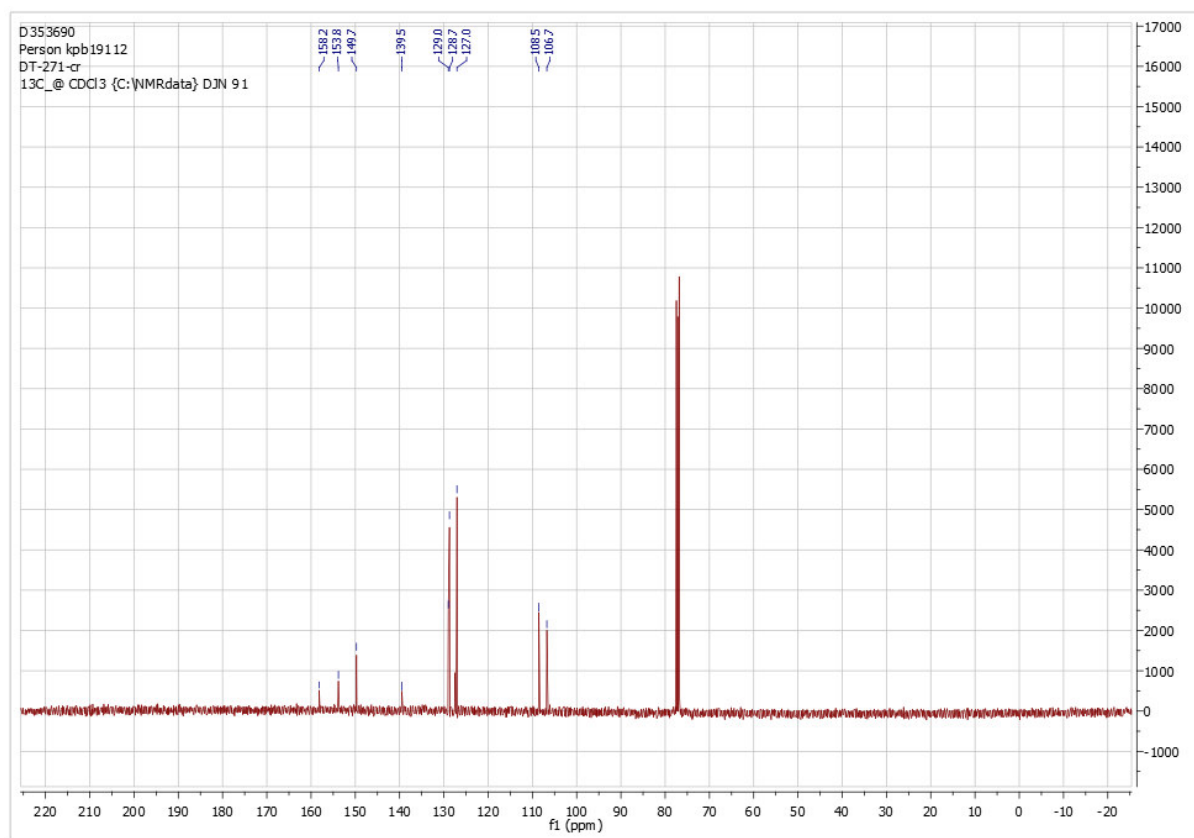
4-trifluoromethyl-2-phenylpyridine: ^{19}F



4-amino-2-phenylpyridine: ^1H

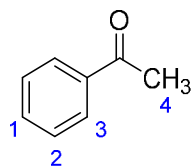


4-amino-2-phenylpyidine: $^{13}\text{C}\{^1\text{H}\}$



Spectral details for unlabelled substrates used in this work:

Acetophenone

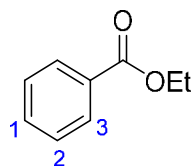


$^1\text{H NMR}$ (400 MHz, CDCl_3) δ = 7.99 – 7.93 (m, 2H, H-3), 7.60 – 7.53 (m, 1H, H-1), 7.51 – 7.42 (m, 2H, H-2), 2.61 (s, 3H, H-4).

Incorporation expected at δ 7.99 – 7.93 ppm (H-3)

Determined against integral at δ 2.61 ppm (H-4)

Ethylbenzoate

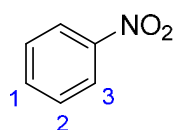


$^1\text{H NMR}$ (400 MHz, CDCl_3) δ = 8.08 – 8.02 (m, 2H, H-3), 7.58 – 7.52 (m, 1H, H-1), 7.47 – 7.40 (m, 2H, H-2), 4.38 (q, J = 7.1 Hz, 2H, CH_2), 1.40 (t, J = 7.1 Hz, 3H, CH_3).

Incorporation expected at δ 8.07 – 8.03 ppm (H-3)

Determined against integral at δ 4.38 ppm (OCH_2CH_3)

Nitrobenzene

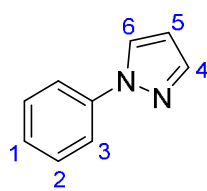


$^1\text{H NMR}$ (400 MHz, CDCl_3) δ = 8.26 – 8.20 (m, 2H, H-3), 7.73 – 7.66 (m, 1H, H-1), 7.58 – 7.51 (m, 2H, H-2).

Incorporation expected at δ 8.26 – 8.20 ppm (H-3)

Determined against integral at δ 7.73 – 7.66 ppm (H-1)

1-phenylpyrazole

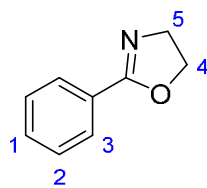


$^1\text{H NMR}$ (400 MHz, CDCl_3) δ = 7.92 (d, J = 2.2 Hz, 1H, H-6), 7.75 – 7.68 (m, 3H, H-3 and H-4), 7.48 – 7.43 (m, 2H, H-2), 7.32 – 7.26 (m, 1H, H-1), 6.49 – 6.45 (m, 1H, H-5).

Incorporation expected at δ 7.75 – 7.68 ppm (H-3)

Determined against integral at δ 7.92 ppm (H-6)

2-phenyloxazoline

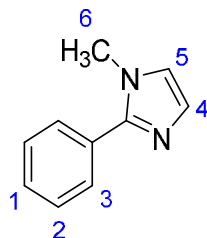


$^1\text{H NMR}$ (400 MHz, CDCl_3) δ = 7.97 – 7.93 (m, 2H, H-3), 7.50 – 7.44 (m, 1H, H-1), 7.43 – 7.37 (m, 2H, H-2), 4.43 (t, J = 9.5 Hz, 2H, H-4), 4.06 (t, J = 9.5 Hz, 2H, H-5).

Incorporation expected at δ 7.97 – 7.93 ppm (H-3)

Determined against integral at δ 4.43 ppm (H-4)

1-methyl-2-phenylimidazole

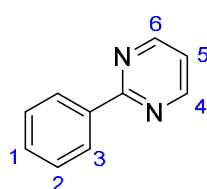


$^1\text{H NMR}$ (400 MHz, CDCl_3) δ = 7.65 – 7.60 (m, 2H, H-3), 7.47 – 7.34 (m, 3H, H-1 and H-2), 7.12 (d, J = 1.2 Hz, 1H, H-5), 6.97 (d, J = 1.2 Hz, 1H, H-4), 3.19 (s, 3H, H-6).

Incorporation expected at δ 7.65 – 7.60 ppm (H-3)

Incorporation determined against δ 7.12 ppm (H-5)

2-phenylpyrimidine

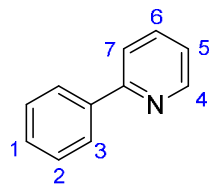


$^1\text{H NMR}$ (400 MHz, CDCl_3): δ 8.81 (d, 2H, J = 4.9 Hz, H-4), 8.48 – 8.43 (m, 2H, H-3), 7.52 – 7.48 (m, 3H, H-1 and H-2), 7.18 (t, 1H, J = 4.9 Hz, H-5)

Incorporation expected at δ 8.48 – 8.43 ppm (H-3)

Determined against integral at δ 7.18 ppm (H-5)

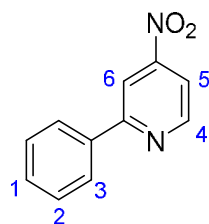
2-phenylpyridines



¹H NMR (400 MHz, CDCl₃) δ = 8.73 – 8.67 (m, 1H, H-4), 8.02 – 7.98 (m, 2H, H-3), 7.78 – 7.70 (m, 2H, H-6 and H-7), 7.51 – 7.45 (m, 2H, H-2), 7.45 – 7.39 (m, 1H, H-1), 7.25 – 7.21 (m, 1H, H-5).

Incorporation expected at δ 8.02 – 7.98 ppm (H-3)

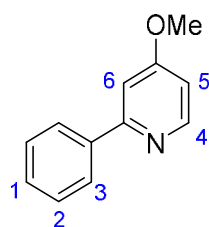
Determined against integral at δ 8.73 – 8.67 ppm (H-4)



¹H NMR (400 MHz, CDCl₃) δ 8.97 (d, *J* = 5.3 Hz, 1H, H-4), 8.45 (d, *J* = 1.7 Hz, 1H, H-6), 8.12 – 8.06 (m, 2H, H-3), 7.94 (dd, *J* = 5.3, 2.0 Hz, 1H, H-5), 7.59 – 7.48 (m, 3H, H-1 and H-2).

Incorporation expected at δ 8.12 – 8.06 ppm (H-3)

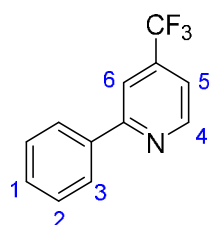
Determined against integral at δ 8.97 (d, *J* = 5.3 Hz, 1H, H-4)



¹H NMR (400 MHz, CDCl₃) δ 8.52 (d, *J* = 5.7 Hz, 1H, H-4), 7.98 – 7.94 (m, 2H, H-3), 7.50 – 7.38 (m, 3H, H-1 and H-2), 7.23 (d, *J* = 2.4 Hz, 1H, H-6), 6.77 (dd, *J* = 5.7, 2.4 Hz, 1H, H-5), 3.90 (s, 3H, Me).

Incorporation expected at δ 7.98 – 7.94 ppm (H-3)

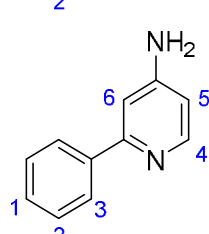
Determined against integral at δ 6.77 ppm (H-5)



¹H NMR (400 MHz, CDCl₃) δ 8.87 (d, *J* = 5.1 Hz, 1H, H-4), 8.07 – 7.99 (m, 2H, H-3), 7.95 – 7.91 (m, 1H, H-6), 7.55 – 7.42 (m, 4H, H-1, H-2 and H-5).

Incorporation expected at δ 8.07 – 7.99 (H-3)

Determined against integral at δ 8.87 (H-4)



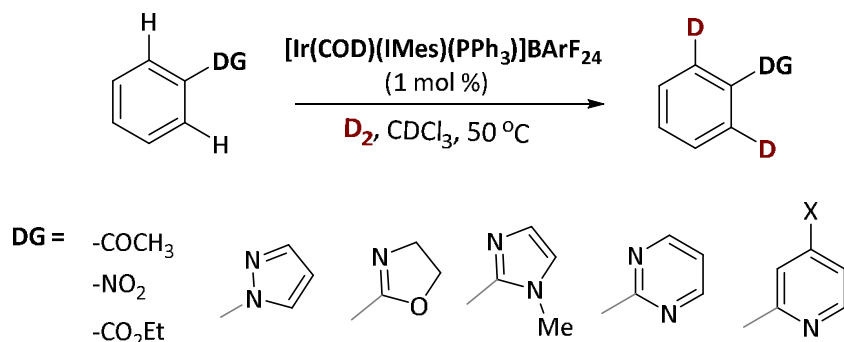
¹H NMR (400 MHz, CDCl₃) δ 8.26 (d, *J* = 5.6 Hz, 1H, H-4), 7.83 – 7.90 (m, 2H, H-3), 7.45 – 7.37 (m, 3H, H-1 and H-2), 6.91 (d, *J* = 2.1 Hz, 1H, H-6), 6.46 (dd, *J* = 5.6, 2.2 Hz, 1H, H-5).

Incorporation expected at δ 7.83 – 7.90 (H-3)

Determined against integral at δ 8.26 (H-4)

3. Kinetic data

3.1. General Kinetic Protocol for reaction monitoring by sampling



Ph-DG (0.50 mmol) and the iridium(I) pre-catalyst (0.005 mmol) were weighed into small vials. The solids were directly transferred to the reaction vial; any liquid substrates were first dissolved in a small amount of CDCl_3 , the vial was washed with solvent, and the washings were transferred to the reaction vial. The reaction mixture was diluted using 2.5 mL (in total) of CDCl_3 ($[\text{Ph-DG}]_0 = 0.20 \text{ mol/L}$). An aliquot was withdrawn to measure the initial spectrum and the vial was capped.

The solution was cooled in an acetone/dry ice bath and the headspace of the vial was evacuated and then refilled with deuterium gas (1 atm) from the balloon. After 3 vacuum/deuterium cycles, the reaction vial was removed from the cooling bath and placed in an aluminum block or thermostat-controlled water bath that had been preheated to 50 °C and the timer was started. The reaction mixture was then stirred vigorously (860 rpm) at 50 °C for 1-2 mins, allowing for catalyst activation and temperature equilibrium before the first aliquot was taken. The deuterium balloon was left in place for the duration of the reaction to ensure a continuous supply (and an excess) of D_2 .

The aliquots (0.04 mL) of reaction mixture were removed at the specified intervals throughout the reaction *via* syringe to an NMR tube and diluted with 0.5 mL of CDCl_3 . For GC-MS: the aliquots (0.005 mL) taken from the reaction were diluted with CHCl_3 prior to the analysis. For LC-MS: the CDCl_3 from the aliquots (0.005 mL) taken from the reaction was evaporated and the residue was dissolved in an acetonitrile/water mixture.

3.2. Mass spectrometry analysis for isotopologue distribution over time.

The distribution of d_0 , d_1 , and d_2 isotopologues in the products was determined by a liquid chromatography-mass spectrometry (LC-MS) for heterocyclic DGs and gas chromatography-mass spectrometry (GC-MS) for acetophenone, nitrobenzene and ethyl benzoate by analysing the aliquots taken from the HIE reactions performed following general procedure.

The distribution of d_0 , d_1 , and d_2 substrates was determined from the corresponding normalised relative abundances at peaks of [M] (d_0), [M+1] (d_1), [M+2] (d_2) for GC-MS and at peaks [M+H] (d_0), [M+H+1] (d_1), [M+H+2] (d_2) for positive ion mode LC-MS analysis for all the heterocyclic substrates apart from 4-nitro-2-phenylpyridine where the negative ion mode was used to determine the relative abundances at peaks of [M-H] (d_0), [M-H+1] (d_1), [M-H+2] (d_2).

The observed relative isotopic abundances were corrected with regard to the amount of ^{13}C isotope (1.1 % natural abundance). The normalised abundances were obtained by dividing those relative numbers by the total abundance.

The overall level of deuterium incorporation in each substrate was determined according to Equation 1, using the relative peak abundances (d_0 , d_1 , or d_2) for each substrate:

$$\% \text{ Deuteration} \text{ (mass spectrometry)} = (0.5 \times d_1) + d_2 \quad (1)$$

The values were in good agreement with those obtained from ^1H NMR spectra (calculated using Equation 2).

$$\% \text{ Deuteration} \text{ (NMR)} = 100 - [\left(\frac{\text{residual integral}}{\text{number of labelling sites}} \right) \times 100] \quad (2)$$

The levels of deuterium incorporation derived from both methods are in good agreement.

Table S1. The extent of deuterium labelling and the distribution of d_0 , d_1 , and d_2 in acetophenone as determined by GC-MS analysis.

Following the General Kinetic Protocol using 60.1 mg of acetophenone, 8.7 mg of Ir-catalyst.

Observed relative abundances									
		m/z	Ph(H ₂)DG	10 min	20 min	30 min	60 min	90 min	120 min
M	d_0	120	100.0	100.0	80.5	37.6	35.0	21.9	15.8
M+1	d_1	121	8.8	35.5	100.0	100.0	100.0	94.6	79.8
M+2	d_2	122	0.6	9.0	29.6	53.0	79.7	100.0	100.0
Relative abundances adjusted for natural abundance of isotopes									
		m/z	Ph(H ₂)DG	10 min	20 min	30 min	60 min	90 min	120 min
M	d_0	120	100.0	100.0	100.0	100.0	35.0	21.9	15.8
M+1	d_1	121	0.0	26.5	92.8	96.6	96.9	92.6	78.4
M+2	d_2	122	0.0	4.8	19.8	43.6	70.4	91.3	92.7
Total abundance			100.0	131.3	212.5	240.3	202.2	205.8	186.8
Normalised relative abundances									
		m/z	Ph(H ₂)DG	10 min	20 min	30 min	60 min	90 min	120 min
M	d_0	120	100.0	76.1	47.0	41.6	17.3	10.6	8.5
M+1	d_1	121	0.0	20.2	43.6	40.2	47.9	45.0	41.9
M+2	d_2	122	0.0	3.6	9.3	18.2	34.8	44.4	49.6
Level of deuterium incorporation									
		Ph(H ₂)DG	10 min	20 min	30 min	60 min	90 min	120 min	
%D by GC-MS		0	14	31	38	59	67	71	
%D by NMR		0	18	32	44	60	67	71	

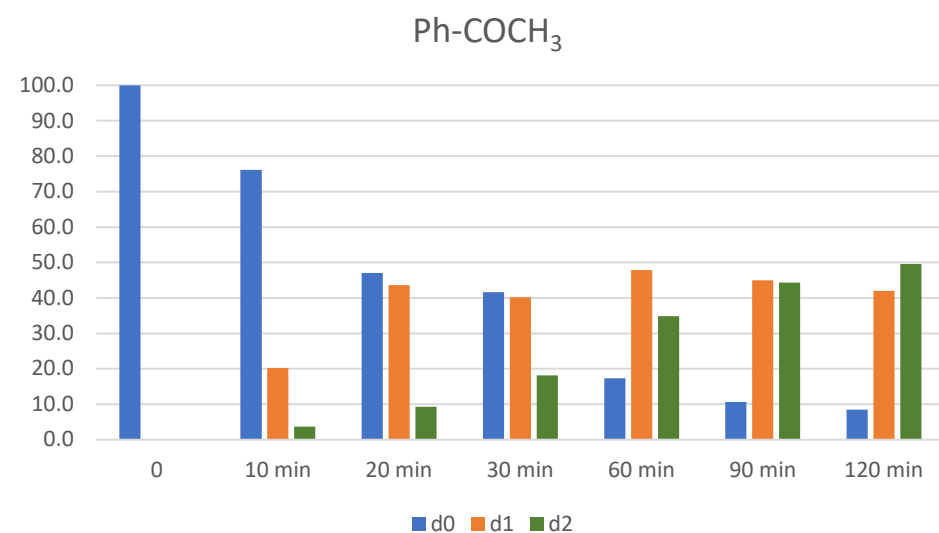


Figure S1. The distribution of d_0 , d_1 , and d_2 during acetophenone labelling as determined by GC-MS analysis.

Table S2. The extent of deuterium labelling and the distribution of d_0 , d_1 , and d_2 in nitrobenzene as determined by GC-MS analysis.

Following the General Kinetic Protocol using 61.5 mg of nitrobenzene, 8.7 mg of Ir-catalyst.

Observed relative abundances												
		m/z	Ph(H ₂)DG	5 min	10 min	20 min	30 min	60 min	90 min	120 min	180 min	270 min
M	d_0	123	100.0	100.0	100.0	100.0	98.9	57.7	34.5	28.2	11.2	8.1
M+1	d_1	124	7.1	32.6	41.2	66.6	100.0	100.0	100.0	100.0	81.8	62.4
M+2	d_2	125	0.8	3.5	5.9	13.9	24.8	40.8	64.3	89.7	100.0	100.0
Relative abundances adjusted for natural abundance of isotopes												
		m/z	Ph(H ₂)DG	5 min	10 min	20 min	30 min	60 min	90 min	120 min	180 min	270 min
M	d_0	123	100.0	100.0	100.0	100.0	98.9	57.7	34.5	28.2	11.2	8.1
M+1	d_1	124	0.0	25.5	34.1	59.5	93.0	95.9	97.6	98.0	81.0	61.8
M+2	d_2	125	0.0	0.4	2.2	8.4	17.0	33.4	57.1	82.5	94.2	95.6
Total abundance		100.0	126.0	136.3	168.0	208.9	187.0	189.1	208.7	186.5	165.5	
Normalised relative abundances												
	%	m/z	Ph(H ₂)DG	5 min	10 min	20 min	30 min	60 min	90 min	120 min	180 min	270 min
M	d_0	123	100.0	79.4	73.4	59.5	47.4	30.8	18.2	13.5	6.0	4.9
M+1	d_1	124	0.0	20.3	25.0	35.4	44.5	51.3	51.6	47.0	43.5	37.3
M+2	d_2	125	0.0	0.3	1.6	5.0	8.1	17.9	30.2	39.5	50.5	57.8
Level of deuterium incorporation												
		Ph(H ₂)DG	5 min	10 min	20 min	30 min	60 min	90 min	120 min	180 min	270 min	
%D by GC-MS		0	10	14	23	30	43	56	63	72	76	
%D by NMR		0	12	16	24	31	45	56	63	71	76	

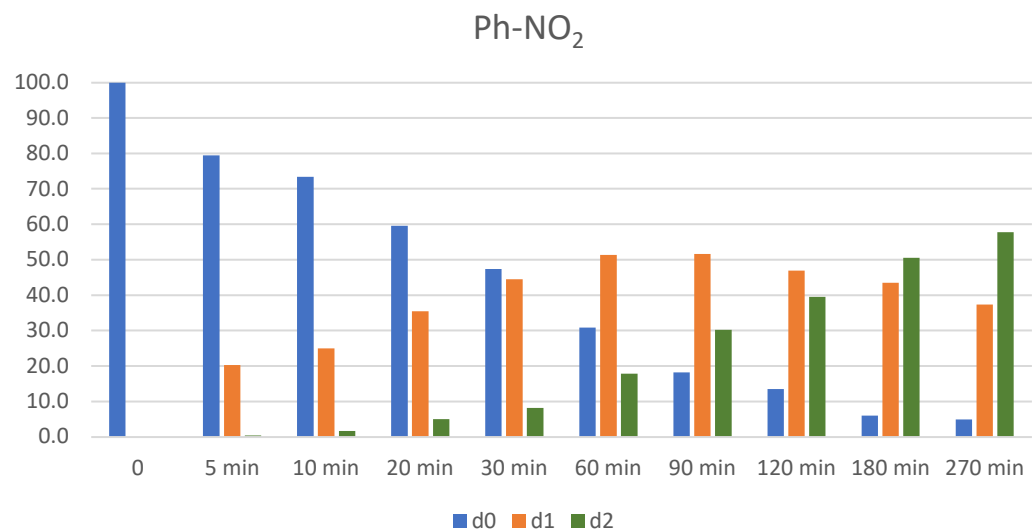


Figure S2. The distribution of d_0 , d_1 , and d_2 during nitrobenzene labelling as determined by GC-MS analysis.

Table S3. The extent of deuterium labelling and the distribution of d_0 , d_1 , and d_2 in ethyl benzoate as determined by GC-MS analysis.

Following the General Kinetic Protocol using 75.1 mg of ethyl benzoate, 8.7 mg of Ir-catalyst.

Observed relative abundances										
		m/z	Ph(H ₂)DG	10 min	20 min	30 min	60 min	90 min	120 min	200 min
M	d_0	150	100.0	100.0	100.0	100.0	54.2	43.1	23.1	24.5
M+1	d_1	151	9.9	37.7	68.6	102.0	100.0	100.0	100.0	100.0
M+2	d_2	152	0.6	5.8	16.4	31.0	56.7	68.1	95.4	166.2
Relative abundances adjusted for natural abundance of isotopes										
		m/z	Ph(H ₂)DG	10 min	20 min	30 min	60 min	90 min	120 min	200 min
M	d_0	150	100.0	100.0	100.0	100.0	54.2	43.1	23.1	24.5
M+1	d_1	151	0.0	27.7	58.6	92.0	94.6	95.7	97.7	97.6
M+2	d_2	152	0.0	1.1	8.5	19.8	46.1	57.6	85.2	156.0
Total abundance			100.0	128.7	167.1	211.9	194.9	196.4	206.0	278.0
Normalised relative abundances										
		m/z	Ph(H ₂)DG	10 min	20 min	30 min	60 min	90 min	120 min	200 min
M	d_0	150	100.0	77.7	59.8	47.2	27.8	22.0	11.2	8.8
M+1	d_1	151	0.0	21.5	35.1	43.4	48.5	48.7	47.4	35.1
M+2	d_2	152	0.0	0.8	5.1	9.4	23.7	29.3	41.3	56.1
Level of deuterium incorporation										
		Ph(H ₂)DG	10 min	20 min	30 min	60 min	90 min	120 min	200 min	
%D by GC-MS		0	12	23	31	48	54	65	74	
%D by NMR		0	14	25	33	50	58	65	78	

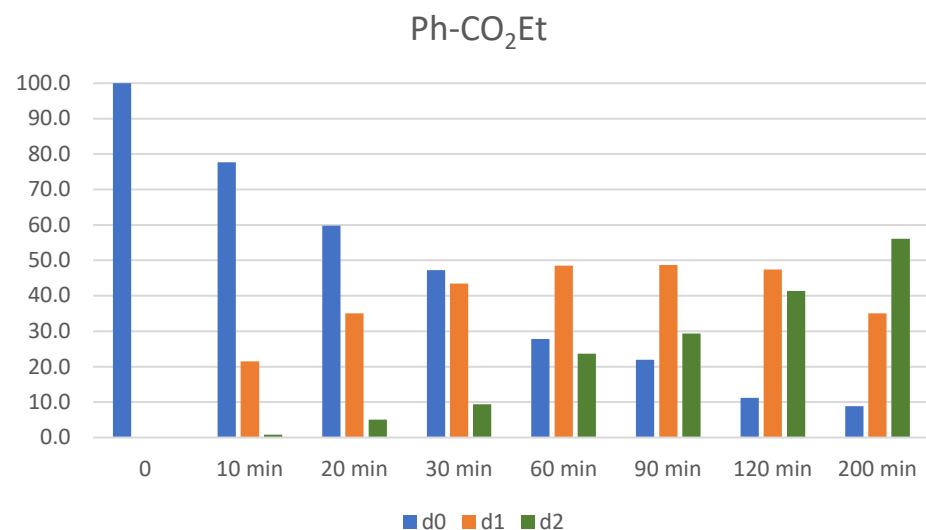


Figure S3. The distribution of d_0 , d_1 , and d_2 during ethyl benzoate labelling as determined by GC-MS analysis.

Table S4. The extent of deuterium labelling and the distribution of d_0 , d_1 , and d_2 in 2-phenylpyridine as determined by LC-MS analysis.

Following the General Kinetic Protocol using 77.6 mg of 2-phenylpyridine, 8.7 mg of Ir-catalyst.

Observed relative abundances									
		m/z	Ph(H ₂)DG	30 min	60 min	90 min	120 min	180 min	240 min
(M+H)	d_0	156	100.0	100.0	100.0	100.0	100.0	52.5	36.6
(M+H)+1	d_1	157	13.3	23.5	34.3	42.2	59.3	51.7	55.0
(M+H)+2	d_2	158	0.9	18.6	43.4	66.1	95.5	100.0	100.0
Relative abundances adjusted for natural abundance of isotopes									
		m/z	Ph(H ₂)DG	30 min	60 min	90 min	120 min	180 min	240 min
(M+H)	d_0	156	100.0	100.0	100.0	100.0	100.0	52.5	36.6
(M+H)+1	d_1	157	0.0	10.2	21.0	28.9	46.0	44.7	50.1
(M+H)+2	d_2	158	0.0	14.6	37.9	59.6	86.7	92.7	92.4
Total abundance			100.0	124.8	158.9	188.5	232.7	189.9	179.1
Normalised relative abundances									
		m/z	Ph(H ₂)DG	30 min	60 min	90 min	120 min	180 min	240 min
(M+H)	d_0	156	100.0	80.1	62.9	53.1	43.0	27.7	20.4
(M+H)+1	d_1	157	0.0	8.2	13.2	15.3	19.8	23.6	28.0
(M+H)+2	d_2	158	0.0	11.7	23.9	31.6	37.3	48.8	51.6
Level of deuterium incorporation									
			Ph(H ₂)DG	30 min	60 min	90 min	120 min	180 min	240 min
%D by LC-MS			0	16	30	39	47	61	66
%D by NMR			0	14	27	37	46	58	67

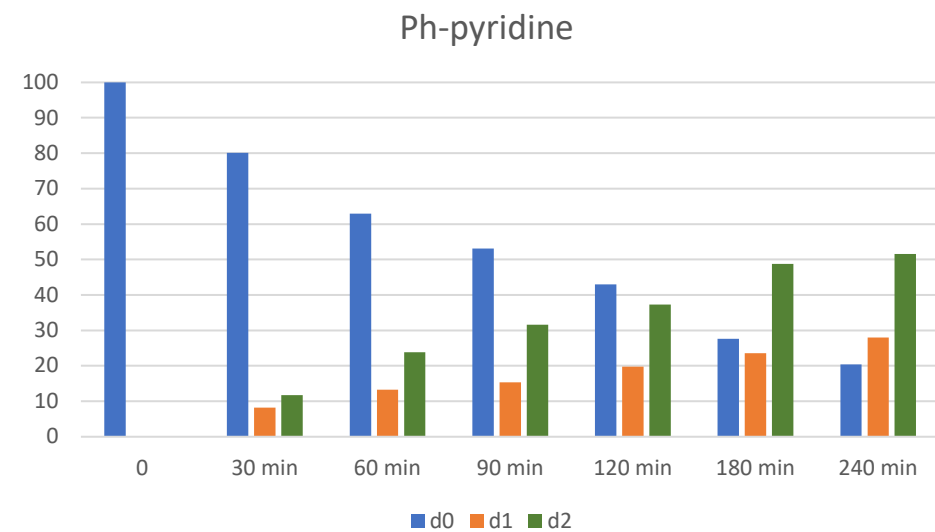


Figure S4. The distribution of d_0 , d_1 , and d_2 during 2-phenylpyridine labelling as determined by LC-MS analysis.

Table S5. The extent of deuterium labelling and the distribution of d_0 , d_1 , and d_2 in 1-methyl-2-phenylimidazole as determined by LC-MS analysis.

Following the General Kinetic Protocol using 79.1 mg of 1-methyl-2-phenylimidazole, 8.7 mg of Ir-catalyst. <i>Observed relative abundances</i>									
		m/z	Ph(H ₂)DG	10 min	20 min	30 min	60 min	90 min	120 min
(M+H)	d_0	159	100.0	100.0	98.7	64.2	29.5	8.8	3.6
(M+H)+1	d_1	160	13.3	49.5	100.0	100.0	100.0	54.2	37.1
(M+H)+2	d_2	161	0.9	10.6	32.8	42.5	90.1	100.0	100.0
<i>Relative abundances adjusted for natural abundance of isotopes</i>									
		m/z	Ph(H ₂)DG	10 min	20 min	30 min	60 min	90 min	120 min
(M+H)	d_0	159	100.0	100.0	98.7	64.2	29.5	8.8	3.6
(M+H)+1	d_1	160	0.0	37.5	88.2	92.3	96.5	53.1	36.7
(M+H)+2	d_2	161	0.0	3.7	19.8	29.9	77.8	93.4	95.5
Total abundance			100.0	141.2	206.7	186.4	203.8	155.4	135.8
<i>Normalised relative abundances</i>									
		m/z	Ph(H ₂)DG	10 min	20 min	30 min	60 min	90 min	120 min
(M+H)	d_0	159	100.0	70.8	47.8	34.5	14.5	5.7	2.7
(M+H)+1	d_1	160	0.0	26.6	42.7	49.5	47.3	34.2	27.0
(M+H)+2	d_2	161	0.0	2.6	9.6	16.0	38.2	60.1	70.3
<i>Level of deuterium incorporation</i>									
			Ph(H ₂)DG	10 min	20 min	30 min	60 min	90 min	120 min
%D by LC-MS			0	16	31	41	62	77	84
%D by NMR			0	11	25	36	57	72	83

1-Me-2-Ph-imidazole

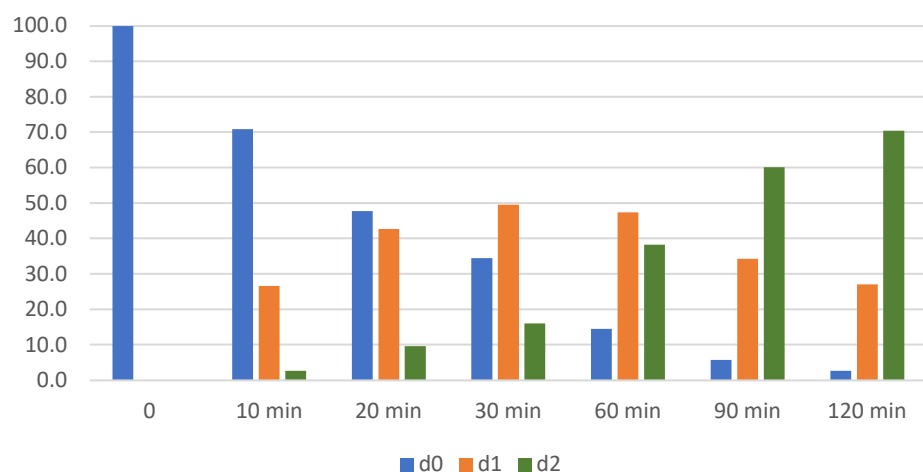


Figure S5. The distribution of d_0 , d_1 , and d_2 during 1-methyl-2-phenylimidazole labelling as determined by LC-MS analysis.

Table S6. The extent of deuterium labelling and the distribution of d_0 , d_1 , and d_2 in 2-phenylpyrimidine as determined by LC-MS analysis.

Following the General Kinetic Protocol using 78.1 mg of 2-phenylpyrimidine, 8.7 mg of Ir-catalyst.

Observed relative abundances											
		m/z	Ph(H ₂)DG	10 min	20 min	30 min	40 min	50 min	60 min	90 min	120 min
(M+H)	d_0	157	100	100.0	100.0	100.0	100.0	100.0	100.0	98.8	63.7
(M+H)+1	d_1	158	11.9	18.7	25.5	34.1	42.4	50.2	69.9	100.0	100.0
(M+H)+2	d_2	159	0.7	8.2	11.7	15.8	25.0	35.3	50.0	97.2	96.3
Relative abundances adjusted for natural abundance of isotopes											
		m/z	Ph(H ₂)DG	10 min	20 min	30 min	40 min	50 min	60 min	90 min	120 min
(M+H)	d_0	157	100.0	100.0	100.0	100.0	100.0	100.0	100.0	98.8	63.7
(M+H)+1	d_1	158	0.0	6.8	13.6	22.2	30.5	38.3	58.0	88.2	92.4
(M+H)+2	d_2	159	0.0	5.3	8.0	11.0	19.3	28.6	41.0	84.6	84.0
Total abundance			100.0	112.1	121.6	133.2	149.8	166.9	199.0	271.7	240.1
Normalised relative abundances											
		m/z	Ph(H ₂)DG	10 min	20 min	30 min	40 min	50 min	60 min	90 min	120 min
(M+H)	d_0	157	100.0	89.2	82.3	75.1	66.8	59.9	50.3	36.4	26.5
(M+H)+1	d_1	158	0.0	6.1	11.2	16.7	20.4	22.9	29.1	32.5	38.5
(M+H)+2	d_2	159	0.0	4.7	6.6	8.3	12.9	17.1	20.6	31.1	35.0
Level of deuterium incorporation											
		Ph(H ₂)DG		10 min	20 min	30 min	40 min	50 min	60 min	90 min	120 min
%D by LC-MS			0	8	12	17	23	29	35	47	54
%D by NMR			0	9	14	17	24	29	35	44	53

Ph-pyrimidine

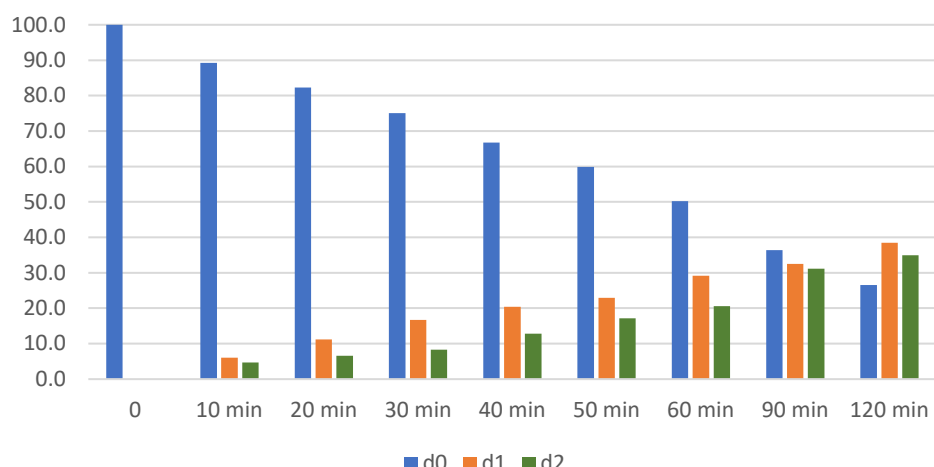


Figure S6. The distribution of d_0 , d_1 , and d_2 during 2-phenylpyrimidine labelling as determined by LC-MS analysis.

Table S7. The extent of deuterium labelling and the distribution of d_0 , d_1 , and d_2 in 2-phenylpyrazole as determined by LC-MS analysis.

Following the General Kinetic Protocol using 72.1 mg of 2-phenylpyrazole, 8.7 mg of Ir-catalyst.

Observed relative abundances								
		m/z	Ph(H ₂)DG	10 min	20 min	30 min	60 min	120 min
(M+H)	d_0	145	100	100.0	63.1	49.2	32.8	22.9
(M+H)+1	d_1	146	11.2	74.4	100.0	100.0	100.0	95.2
(M+H)+2	d_2	147	0.5	13.3	45.6	60.9	94.6	100.0
Relative abundances adjusted for natural abundance of isotopes								
		m/z	Ph(H ₂)DG	10 min	20 min	30 min	60 min	120 min
(M+H)	d_0	145	100.0	100.0	63.1	49.2	32.8	22.9
(M+H)+1	d_1	146	0.0	63.2	92.9	94.5	96.3	92.6
(M+H)+2	d_2	147	0.0	4.5	34.1	49.5	83.2	89.2
Total abundance			100.0	167.7	190.1	193.1	212.4	204.8
Normalised relative abundances								
		m/z	Ph(H ₂)DG	10 min	20 min	30 min	60 min	120 min
(M+H)	d_0	145	100.0	59.6	33.2	25.5	15.4	11.2
(M+H)+1	d_1	146	0.0	37.7	48.9	48.9	45.4	45.2
(M+H)+2	d_2	147	0.0	2.7	17.9	25.6	39.2	43.6
Level of deuterium incorporation								
		Ph(H ₂)DG	10 min	20 min	30 min	60 min	120 min	
%D by LC-MS		0	22	42	50	62	66	
%D by NMR		0	20	36	46	58	62	

Ph-pyrazole

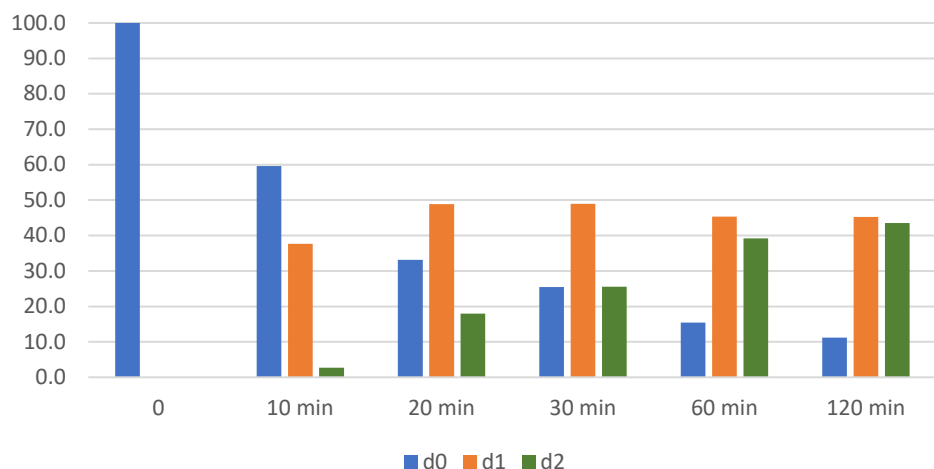


Figure S7. The distribution of d_0 , d_1 , and d_2 during 2-phenylpyrazole labelling as determined by LC-MS analysis.

Table S8. The extent of deuterium labelling and the distribution of d_0 , d_1 , and d_2 in 2-phenyloxazoline as determined by LC-MS analysis.

Following the General Kinetic Protocol using 73.6 mg of 2-phenyloxazoline, 8.7 mg of Ir-catalyst.

Observed relative abundances										
		m/z	Ph(H ₂)DG	5 min	10 min	20 min	30 min	40 min	60 min	80 min
(M+H)	d_0	147	100	100.0	100.0	59.5	40.9	30.6	18.3	14.2
(M+H)+1	d_1	148	10.5	46.9	99.3	100.0	100.0	100.0	84.2	73.6
(M+H)+2	d_2	149	0.8	7.8	28.6	49.4	70.7	84.5	100.0	100.0
Relative abundances adjusted for natural abundance of isotopes										
		m/z	Ph(H ₂)DG	5 min	10 min	20 min	30 min	40 min	60 min	80 min
(M+H)	d_0	147	100	100.0	100.0	59.5	40.9	30.6	18.3	14.2
(M+H)+1	d_1	148	10.5	46.9	99.3	100.0	100.0	100.0	84.2	73.6
(M+H)+2	d_2	149	0.8	7.8	28.6	49.4	70.7	84.5	100.0	100.0
Total abundance			100	100.0	100.0	59.5	40.9	30.6	18.3	14.2
Normalised relative abundances										
		m/z	Ph(H ₂)DG	5 min	10 min	20 min	30 min	40 min	60 min	80 min
(M+H)	d_0	147	100.0	72.2	48.5	31.0	20.8	15.2	9.6	8.0
(M+H)+1	d_1	148	0.0	26.3	43.1	48.9	48.7	48.1	42.9	40.5
(M+H)+2	d_2	149	0.0	1.5	8.4	20.0	30.5	36.7	47.5	51.5
Level of deuterium incorporation										
			Ph(H ₂)DG	5 min	10 min	20 min	30 min	40 min	60 min	80 min
%D by LC-MS			0	15	30	45	55	61	69	72
%D by NMR			0	16	29	44	54	61	67	69

Ph-oxazoline

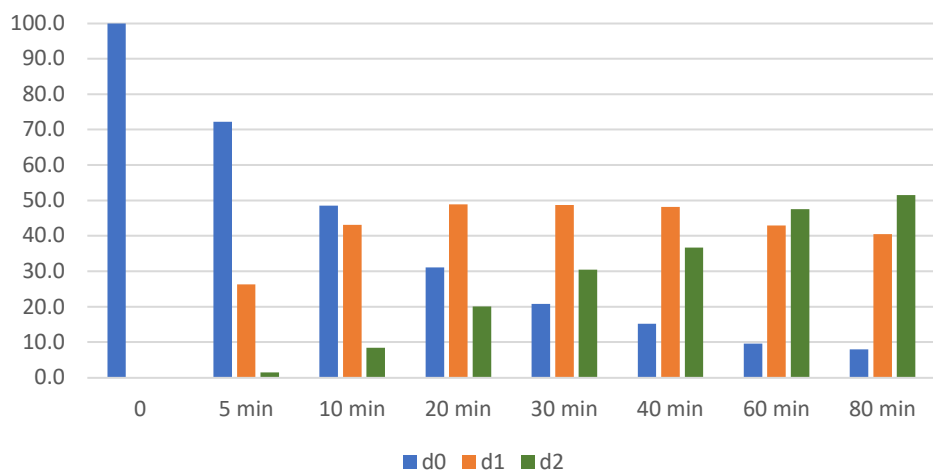


Figure S8. The distribution of d_0 , d_1 , and d_2 during 2-phenyloxazoline labelling as determined by LC-MS analysis.

3.3. Kinetic data and isotopologue distribution for substituted phenylpyridines

Table S9. Rate monitoring for the deuteration of 4-nitro-2-phenyl pyridine.

Following the General Kinetic Protocol using 100.1 mg of 4-nitro-2-phenyl pyridine, 8.7 mg of Ir-catalyst.

Entry	Time, s	Integral (H/D)	[Substrate], M	In [Substrate]
0	0	2.00	0.200	-1.61
1	600	1.76	0.176	-1.74
2	1200	1.67	0.167	-1.79
3	1800	1.57	0.157	-1.85
4	3600	1.34	0.134	-2.01
5	7200	1.04	0.104	-2.26
6	10800	0.82	0.082	-2.50
7	14400	0.69	0.069	-2.67

$k_{\text{obs}} = 1.44 \times 10^{-4} (\text{s}^{-1})$

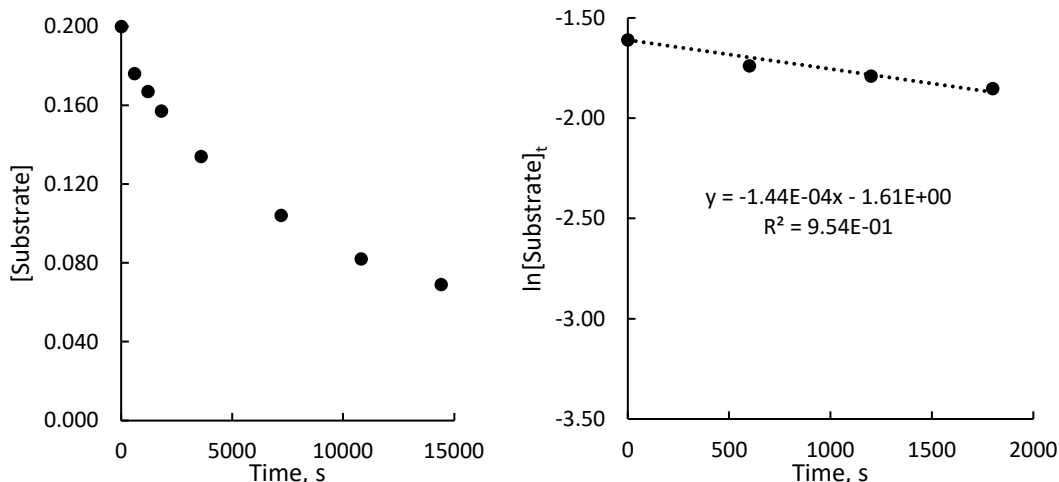


Figure S9 Kinetic profile for the HIE reaction of 4-nitro-2-phenyl pyridine over time in CDCl_3 at 50°C (left). Fitting a first-order kinetic model to the data (right).

Table S10. The extent of deuterium labelling and the distribution of d_0 , d_1 , and d_2 in 4-nitro-2-phenyl pyridine as determined by LC-MS analysis (Data from experiment in Table S9).

Observed relative abundances							
		m/z	Ph(H ₂)DG	60 min	120 min	180 min	240 min
(M-H)	d_0	200	100.0	100.0	50.8	34.8	15.0
(M-H)+1	d_1	201	15.1	98.5	100.0	100.0	94.7
(M-H)+2	d_2	202	1.4	51.7	59.6	93.3	100.0
Relative abundances adjusted for natural abundance of isotopes							
		m/z	Ph(H ₂)DG	60 min	120 min	180 min	240 min
(M-H)	d_0	200	100.0	100.0	50.8	34.8	15.0
(M-H)+1	d_1	201	0.0	83.5	92.4	94.8	92.5
(M-H)+2	d_2	202	0.0	35.5	43.9	77.8	85.6
Total abundance			100.0	219.0	187.1	207.4	193.0
Normalised relative abundances							
		m/z	Ph(H ₂)DG	60 min	120 min	180 min	240 min
(M-H)	d_0	200	100.0	45.0	25.5	17.1	8.2
(M-H)+1	d_1	201	0.0	37.6	46.3	46.6	50.3
(M-H)+2	d_2	202	0.0	16.0	22.0	38.3	46.5
Level of deuterium incorporation							
		Ph(H ₂)DG	60 min	120 min	180 min	240 min	
%D by LC-MS		0	35	45	62	72	
%D by NMR		0	33	48	59	66	

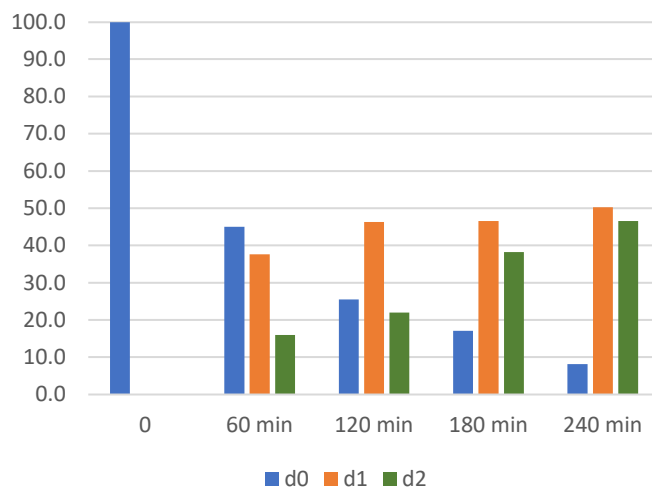
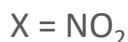


Figure S10. The distribution of d_0 , d_1 , and d_2 during 4-nitro-2-phenyl pyridine labelling as determined by LC-MS analysis.

Table S11. Rate monitoring for the deuteration of 4-methoxy-2-phenyl pyridine.

Following the General Kinetic Protocol using 92.6 mg of 4-methoxy-2-phenyl pyridine, 8.7 mg of Ir-catalyst.

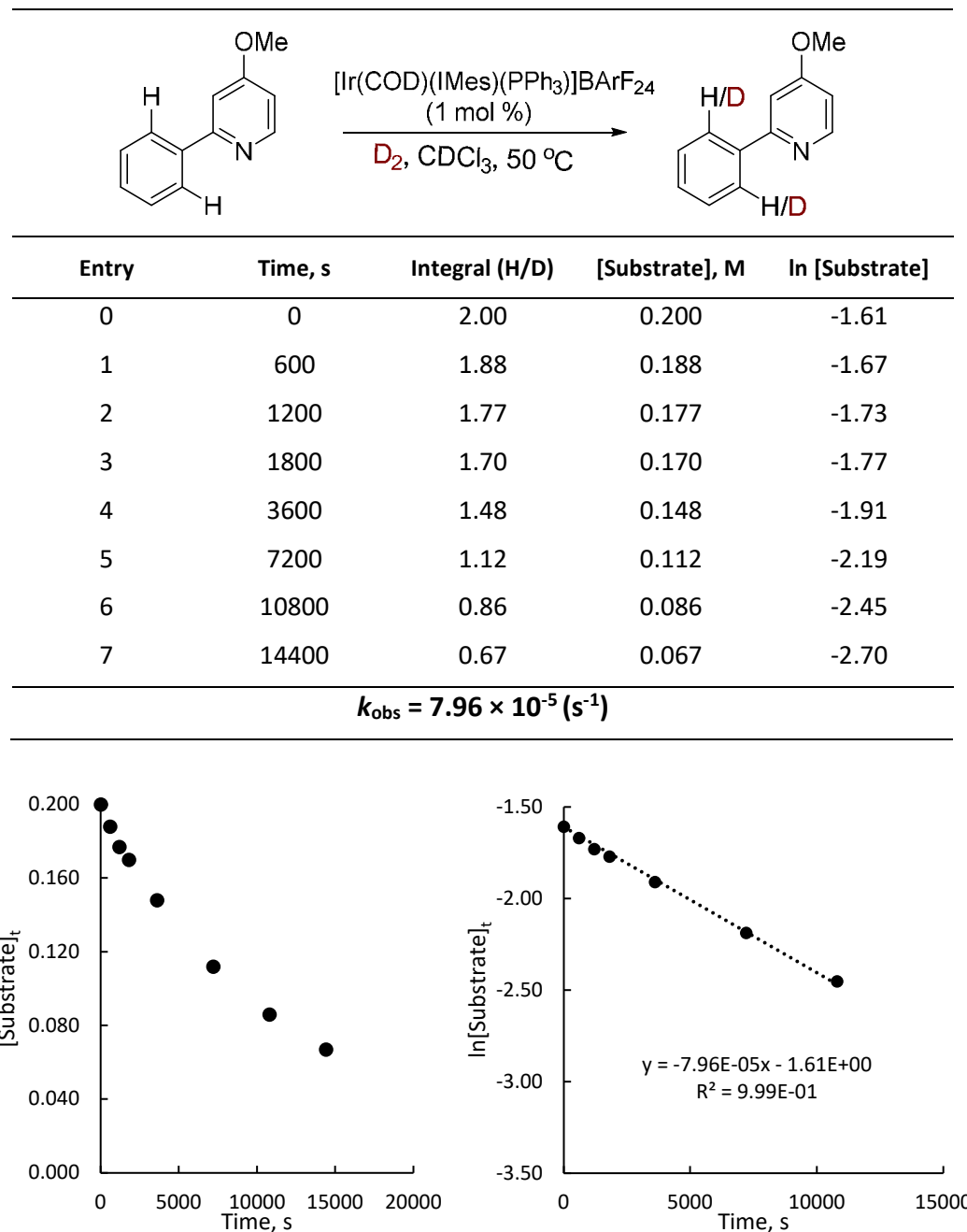


Figure S11. Kinetic profile for the HIE reaction of 4-methoxy-2-phenyl pyridine over time in CDCl_3 at 50 °C (left). Fitting a first-order kinetic model to the data (right).

Table S12. The extent of deuterium labelling and the distribution of d_0 , d_1 , and d_2 in 4-methoxy-2-phenyl pyridine as determined by LC-MS analysis (Data from experiment in Table S11).

Observed relative abundances										
		m/z	Ph(H ₂)DG	10 min	20 min	30 min	60 min	120 min	180 min	240 min
(M+H)	d_0	186	100.0	100.0	100.0	100.0	100.0	100.0	55.0	27.2
(M+H)+1	d_1	187	14.1	17.0	18.2	20.2	27.5	63.8	75.9	68.3
(M+H)+2	d_2	188	1.2	5.9	10.3	16.3	31.7	90.7	100.0	100.0
Relative abundances adjusted for natural abundance of isotopes										
		m/z	Ph(H ₂)DG	10 min	20 min	30 min	60 min	120 min	180 min	240 min
(M+H)	d_0	186	100.0	100.0	100.0	100.0	100.0	100.0	55.0	27.2
(M+H)+1	d_1	187	0.0	2.9	4.1	6.1	13.4	49.7	68.1	64.5
(M+H)+2	d_2	188	0.0	2.3	6.6	12.3	26.7	80.6	88.7	90.1
Total abundance			100.0	105.2	110.7	118.4	140.1	230.3	211.9	181.8
Normalised relative abundances										
		m/z	Ph(H ₂)DG	10 min	20 min	30 min	60 min	120 min	180 min	240 min
(M+H)	d_0	186	100.0	95.0	90.4	84.5	71.4	43.4	26.0	15.0
(M+H)+1	d_1	187	0.0	2.8	3.7	5.2	9.6	21.6	32.2	35.5
(M+H)+2	d_2	188	0.0	2.2	5.9	10.4	19.0	35.0	41.9	49.6
Level of deuterium incorporation										
		Ph(H ₂)DG	10 min	20 min	30 min	60 min	120 min	180 min	240 min	
%D by LC-MS		0	4	8	13	24	46	58	67	
%D by NMR		0	6	12	15	26	44	57	67	

X = OMe

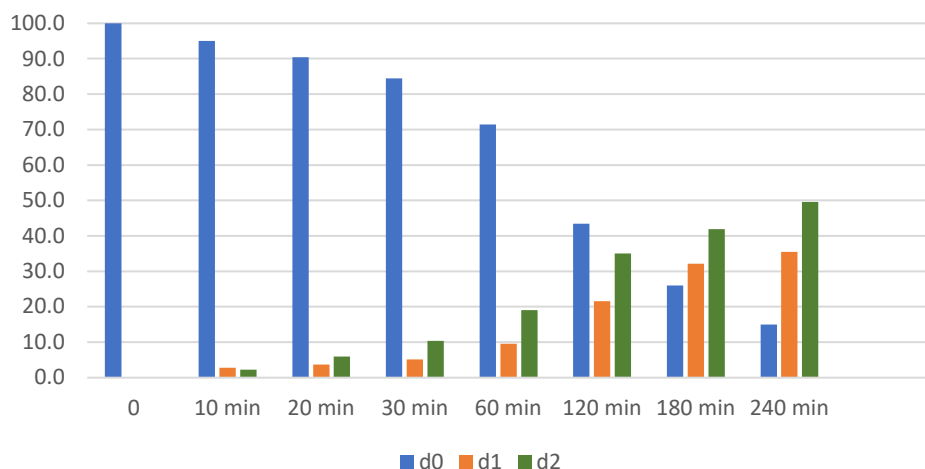


Figure S12. The distribution of d_0 , d_1 , and d_2 during 4-methoxy-2-phenyl pyridine labelling as determined by LC-MS analysis.

Table S13. Rate monitoring for the deuteration of 4-amino-2-phenyl pyridine.

Following the General Kinetic Protocol using 85.1 mg of 4-amino-2-phenyl pyridine, 8.7 mg of Ir-catalyst.

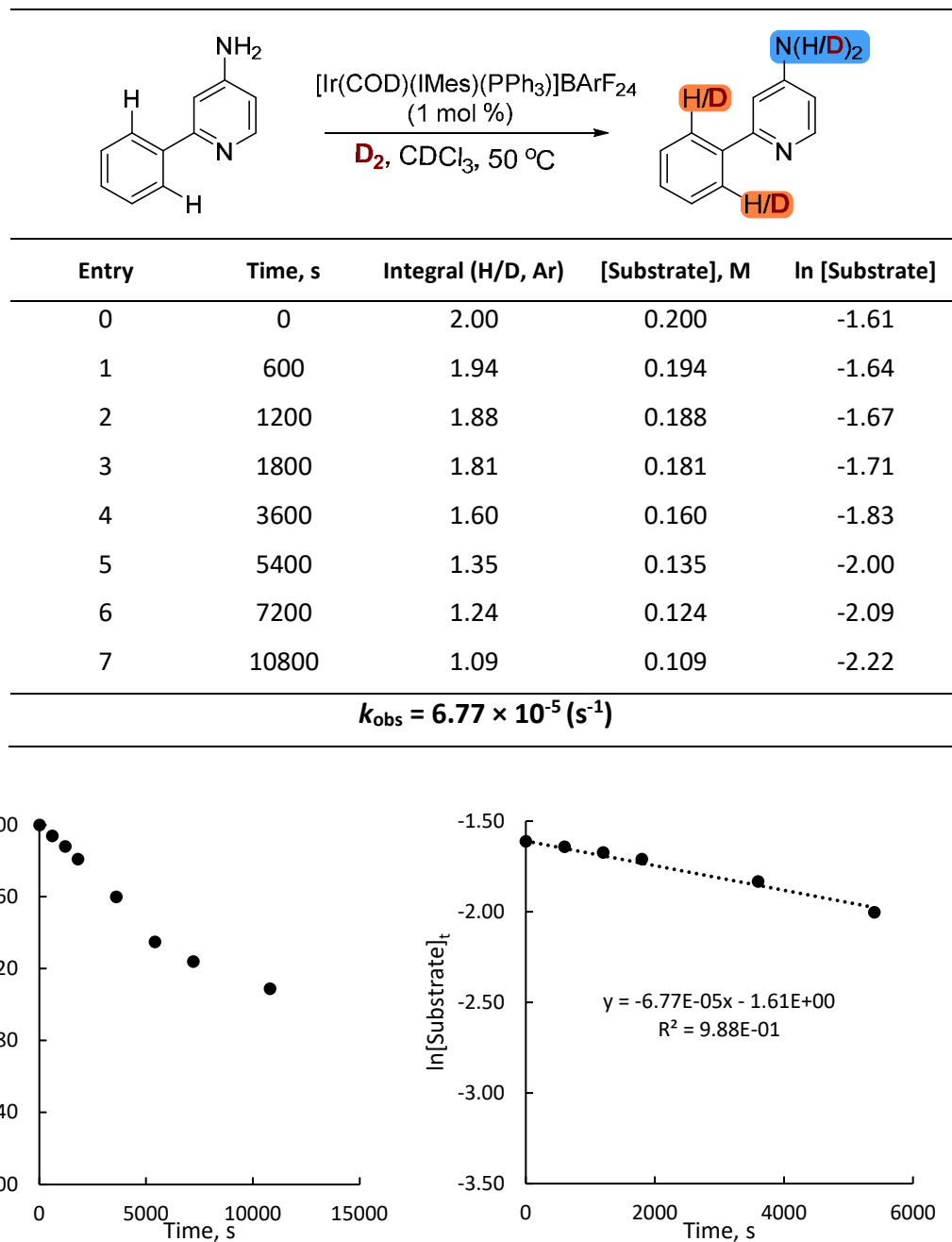
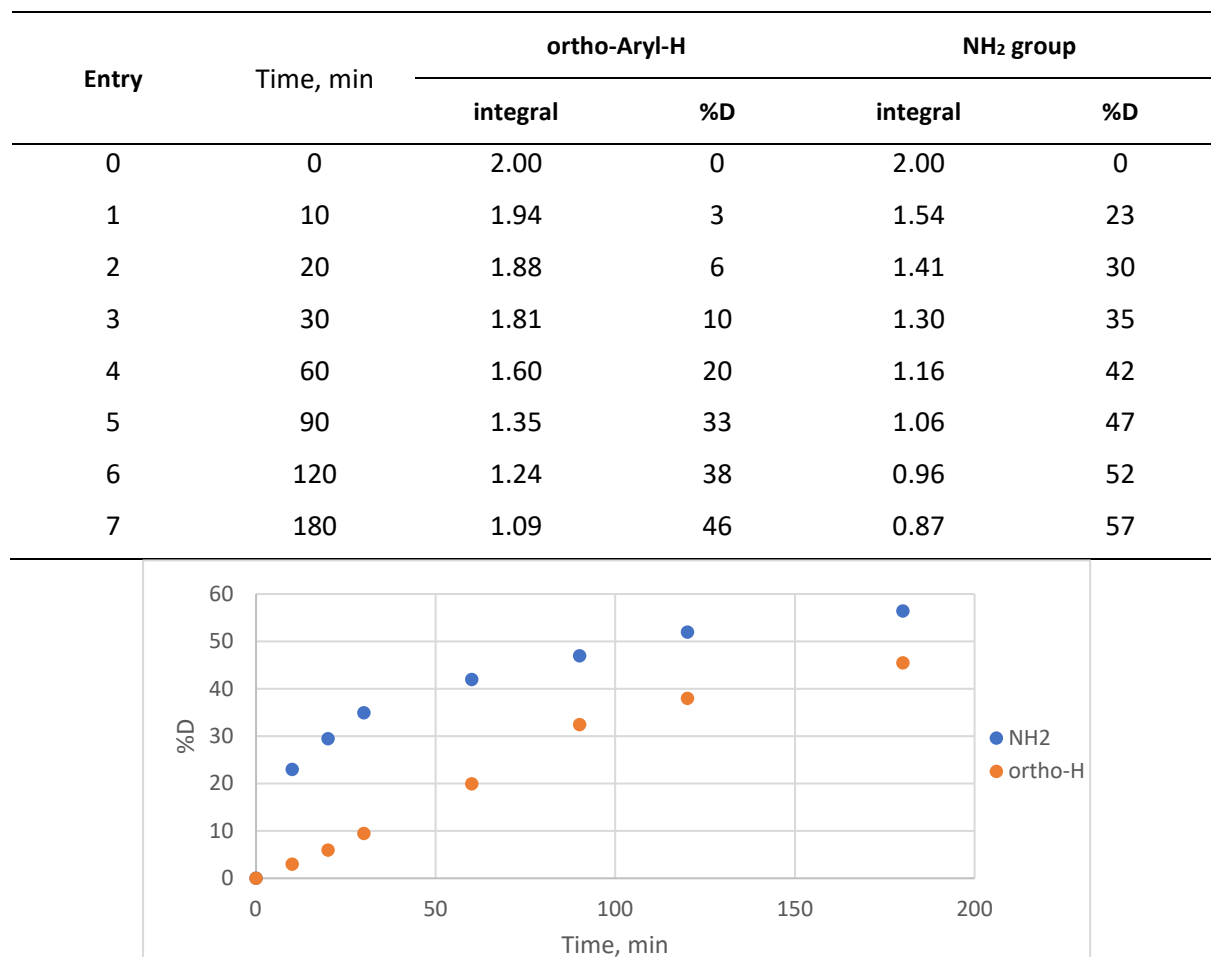


Figure S13. Kinetic profile for the HIE reaction of 4-amino-2-phenyl pyridine over time in CDCl_3 at 50 $^{\circ}\text{C}$ (left). Fitting a first-order kinetic model to the data (right).

Table S14. Deuterium incorporation in the HIE reaction of 4-amino-2-phenyl pyridine.**Figure S14.** Rate study of the deuteration of 4-amino-2-phenyl-pyridine.**Table S15.** Control experiments.

	Conditions ^a	Integral ortho-H	%D		%D	
			ortho-H	NH ₂	ortho-H	NH ₂
A	Substrate + D ₂ in CDCl ₃	NO catalyst	2.00	0	2.00	0
B	Substrate + Catalyst in CDCl ₃	NO D ₂	2.00	0	2.00	0
C	(Catalyst in CDCl ₃) -> vac/D ₂ -> freeze -> vac/Argon -> r.t. -> (Substrate in CDCl ₃)	<i>Direct analysis</i>	2.00	0	1.70	15
	CDCl ₃ evaporated and fresh used for NMR		2.00	0	1.91	5
D	General HIE procedure	<i>Direct analysis</i>	0.58	71	0.51	75
	CDCl ₃ evaporated and fresh used for NMR		0.57	72	0.97	52

^a Following General HIE procedure using 10mg (0.06 mmol) of the substrate and 5.0 mg (0.003 mmol) of catalyst, unless noted otherwise

Table S16. Rate monitoring for the deuteration of 4-trifluoromethyl-2-phenyl pyridine.

Following the General Kinetic Protocol using 111.6 mg of 4-trifluoromethyl-2-phenyl pyridine, 8.7 mg of Ir-catalyst (run1).

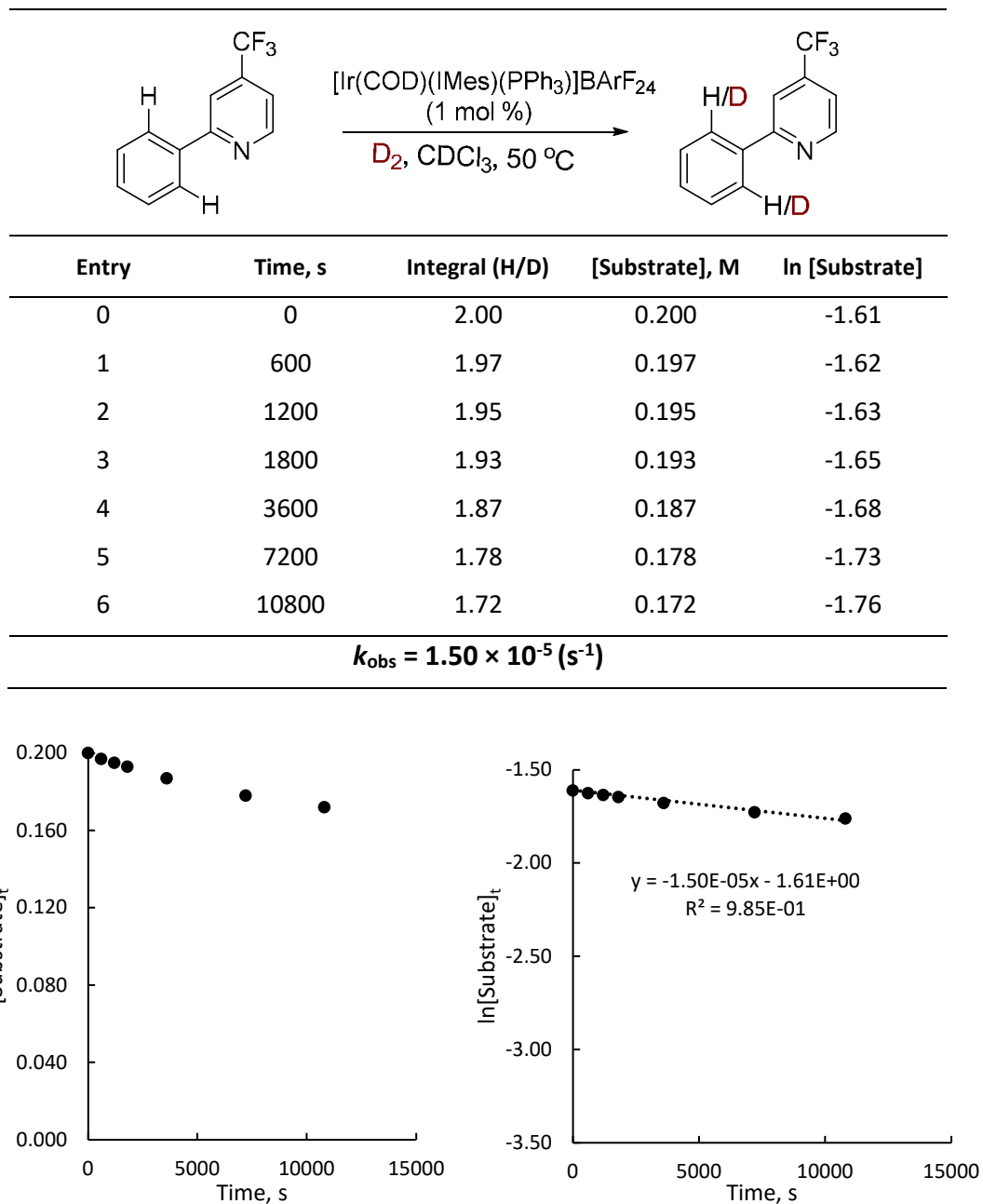


Figure S15. Kinetic profile for the HIE reaction of 4- trifluoromethyl-2-phenyl pyridine over time in CDCl_3 at 50°C (left). Fitting a first-order kinetic model to the data (right).

Table S17. Rate monitoring for the deuteration of 4-trifluoromethyl-2-phenyl pyridine.

Following the General Kinetic Protocol using 111.6 mg of 4-trifluoromethyl-2-phenyl pyridine, 8.7 mg of Ir-catalyst (run 2).

Entry	Time, s	Integral (H/D)	[Substrate], M	ln [Substrate]
0	0	2.00	0.200	-1.61
1	600	1.97	0.197	-1.62
2	1200	1.94	0.194	-1.64
3	1800	1.91	0.191	-1.66
4	3600	1.86	0.186	-1.68
5	7200	1.76	0.176	-1.74
6	10800	1.67	0.167	-1.79
7	14400	1.58	0.158	-1.85
8	18000	1.51	0.151	-1.89

$k_{\text{obs}} = 1.74 \times 10^{-5} (\text{s}^{-1})$

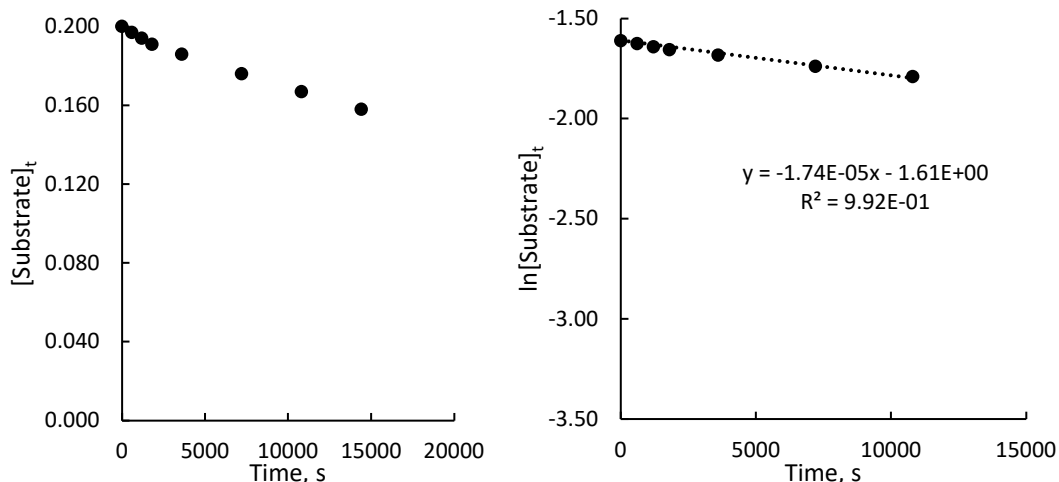


Figure S16. Kinetic profile for the HIE reaction of 4- trifluoromethyl-2-phenyl pyridine over time in CDCl_3 at 50°C (left). Fitting a first-order kinetic model to the data (right).

Table S18. Rate monitoring for the deuteration of 4-trifluoromethyl-2-phenyl pyridine.

Following the General Kinetic Protocol using 111.6 mg of 4-trifluoromethyl-2-phenyl pyridine, 8.7 mg of Ir-catalyst (run 3).

Entry	Time, s	Integral (H/D)	[Substrate], M	In [Substrate]
0	0	2.00	0.200	-1.61
1	600	1.99	0.199	-1.61
2	1200	1.97	0.197	-1.62
3	1800	1.94	0.194	-1.64
4	3600	1.92	0.192	-1.65
5	7200	1.81	0.181	-1.71
6	10800	1.75	0.175	-1.74
7	16200	1.63	0.163	-1.81

$k_{\text{obs}} = 1.26 \times 10^{-5} (\text{s}^{-1})$

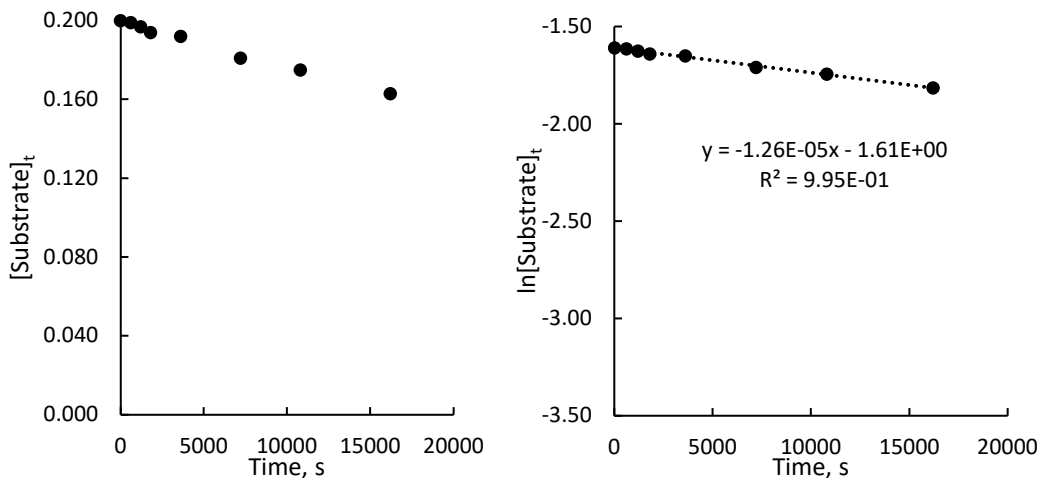


Figure S17. Kinetic profile for the HIE reaction of 4- trifluoromethyl-2-phenyl pyridine over time in CDCl_3 at 50°C (left). Fitting a first-order kinetic model to the data (right).

Table S19. Rate monitoring for the deuteration of 4-trifluoromethyl-2-phenyl pyridine.

Following the General Kinetic Protocol using 111.6 mg of 4-trifluoromethyl-2-phenyl pyridine, 8.7 mg of Ir-catalyst (run 4).

Entry	Time, s	Integral (H/D)	[Substrate], M	In [Substrate]
0	0	2.00	0.200	-1.61
1	600	1.95	0.195	-1.63
2	1200	1.93	0.193	-1.65
3	1800	1.90	0.190	-1.66
4	3600	1.79	0.179	-1.72
5	7200	1.54	0.154	-1.87
6	10800	1.36	0.136	-2.00
7	14400	1.22	0.122	-2.10

$k_{\text{obs}} = 3.48 \times 10^{-5} (\text{s}^{-1})$

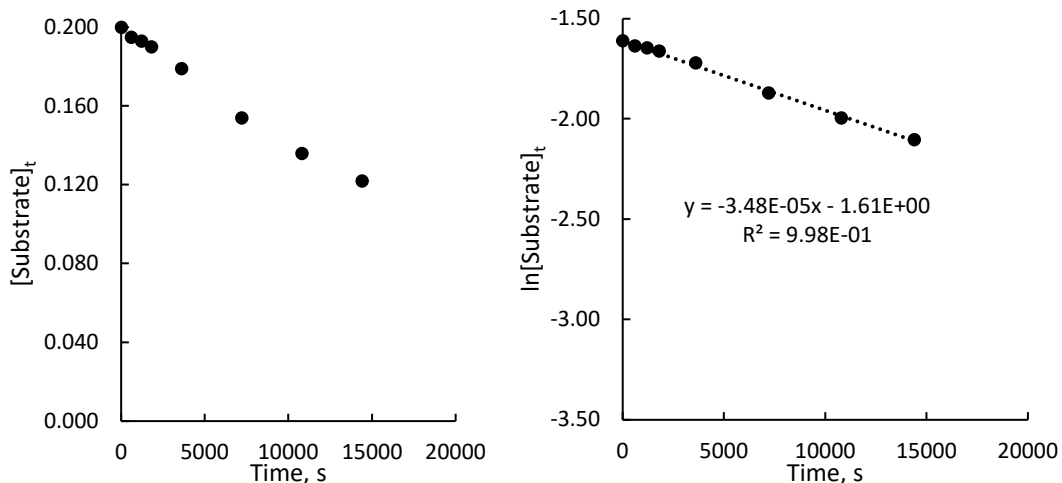


Figure S18. Kinetic profile for the HIE reaction of 4- trifluoromethyl-2-phenyl pyridine over time in CDCl_3 at 50°C (left). Fitting a first-order kinetic model to the data (right).

Table S20. Rate monitoring for the deuteration of 4-trifluoromethyl-2-phenyl pyridine.

Following the General Kinetic Protocol using 85.0 mg (0.38 mmol) of 4-trifluoromethyl-2-phenyl pyridine, 6.9 mg (0.004 mmol) of Ir-catalyst and 2.0 mL of CDCl_3 (run 1).

Entry	Time, s	Integral (H/D)	[Substrate], M	In [Substrate]
0	0	2.00	0.200	-1.61
1	600	1.87	0.187	-1.68
2	1200	1.73	0.173	-1.75
3	1800	1.61	0.161	-1.83
4	3600	1.38	0.138	-1.98
5	7200	1.15	0.115	-2.16
6	10800	1.04	0.104	-2.26

$k_{\text{obs}} = 1.08 \times 10^{-4} (\text{s}^{-1})$

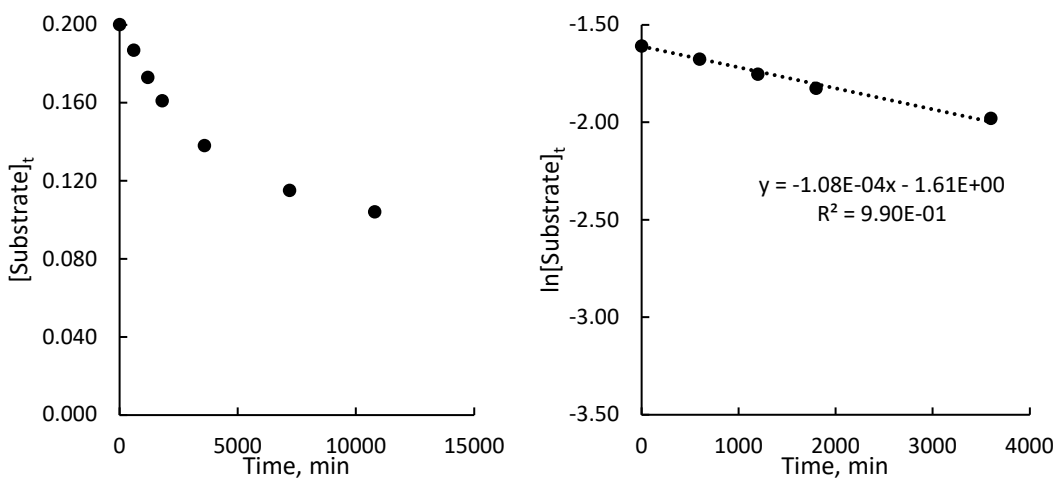


Figure S19. Kinetic profile for the HIE reaction of 4- trifluoromethyl-2-phenyl pyridine over time in CDCl_3 at 50 °C (left). Fitting a first-order kinetic model to the data (right).

Table S21. Rate monitoring for the deuteration of 4-trifluoromethyl-2-phenyl pyridine.

Following the General Kinetic Protocol using 85.0 mg (0.38 mmol) of 4-trifluoromethyl-2-phenyl pyridine, 6.9 mg (0.004 mmol) of Ir-catalyst and 2.0 mL of CDCl_3 (run 2).

Entry	Time, s	Integral (H/D)	[Substrate], M	In [Substrate]
0	0	2.00	0.200	-1.61
1	600	1.89	0.189	-1.67
2	1200	1.76	0.176	-1.74
3	1800	1.65	0.165	-1.80
4	3600	1.34	0.134	-2.01
5	7800	0.99	0.099	-2.31
6	10800	0.83	0.083	-2.49
7	14400	0.75	0.075	-2.59

$k_{\text{obs}} = 1.10 \times 10^{-4} (\text{s}^{-1})$

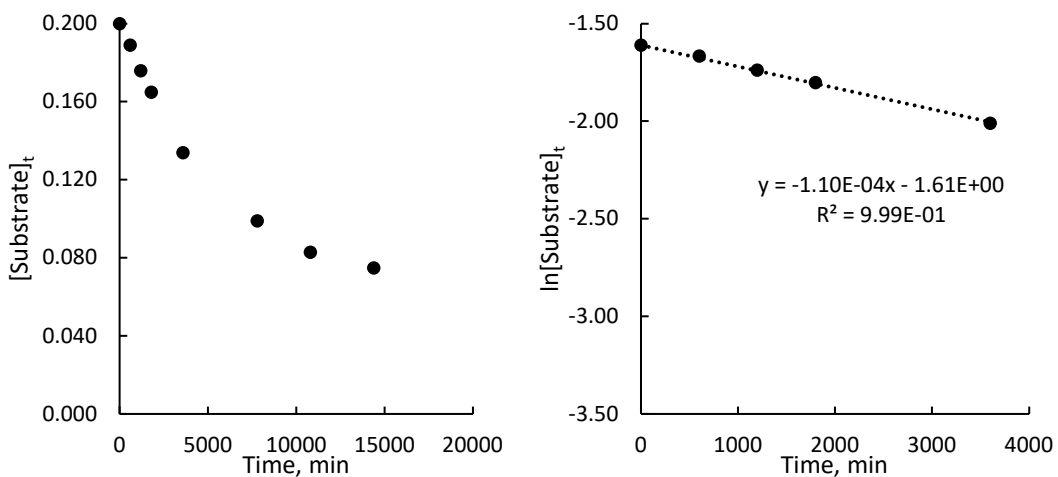


Figure S20. Kinetic profile for the HIE reaction of 4- trifluoromethyl-2-phenyl pyridine over time in CDCl_3 at 50 °C (left). Fitting a first-order kinetic model to the data (right).

Table S22. Rate monitoring for the deuteration of 4-trifluoromethyl-2-phenyl pyridine.

Following the General Kinetic Protocol using 98.2 mg (0.44 mmol) of 4-trifluoromethyl-2-phenyl pyridine, 7.6 mg (0.004 mmol) of Ir-catalyst and 2.2 mL of CDCl_3 (run 1).

Entry	Time, s	Integral (H/D)	[Substrate], M	In [Substrate]
0	0	2.00	0.200	-1.61
1	600	2.00	0.200	-1.61
2	1200	2.00	0.200	-1.61
3	1800	1.98	0.198	-1.62
4	3600	1.90	0.190	-1.66
5	5400	1.84	0.184	-1.69
6	9000	1.70	0.170	-1.77
7	12600	1.55	0.155	-1.86

$k_{\text{obs}} = 1.85 \times 10^{-5} (\text{s}^{-1})$

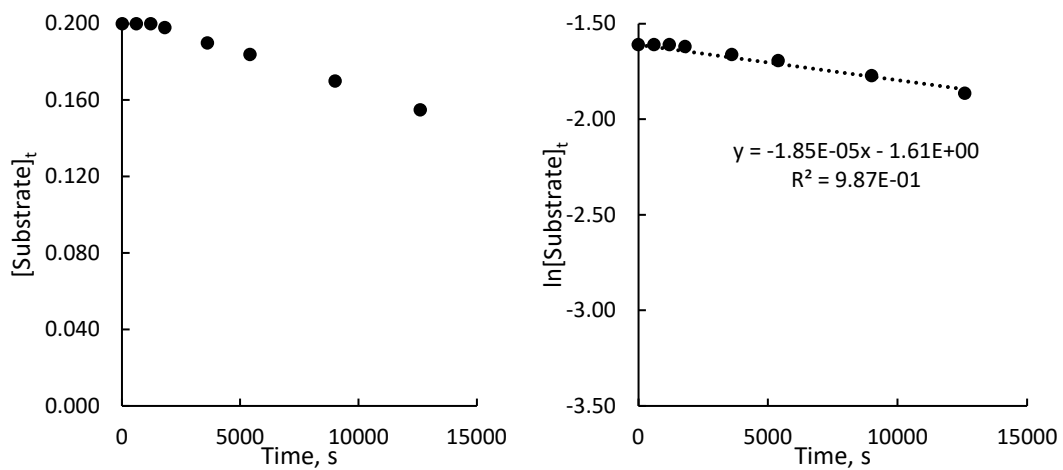


Figure S21. Kinetic profile for the HIE reaction of 4- trifluoromethyl-2-phenyl pyridine over time in CDCl_3 at 50 °C (left). Fitting a first-order kinetic model to the data (right).

Table S23. Rate monitoring for the deuteration of 4-trifluoromethyl-2-phenyl pyridine.

Following the General Kinetic Protocol using 111.6 mg of 4-trifluoromethyl-2-phenyl pyridine, 8.7 mg of Ir-catalyst (catalyst was preactivated with D₂ before substrate addition).

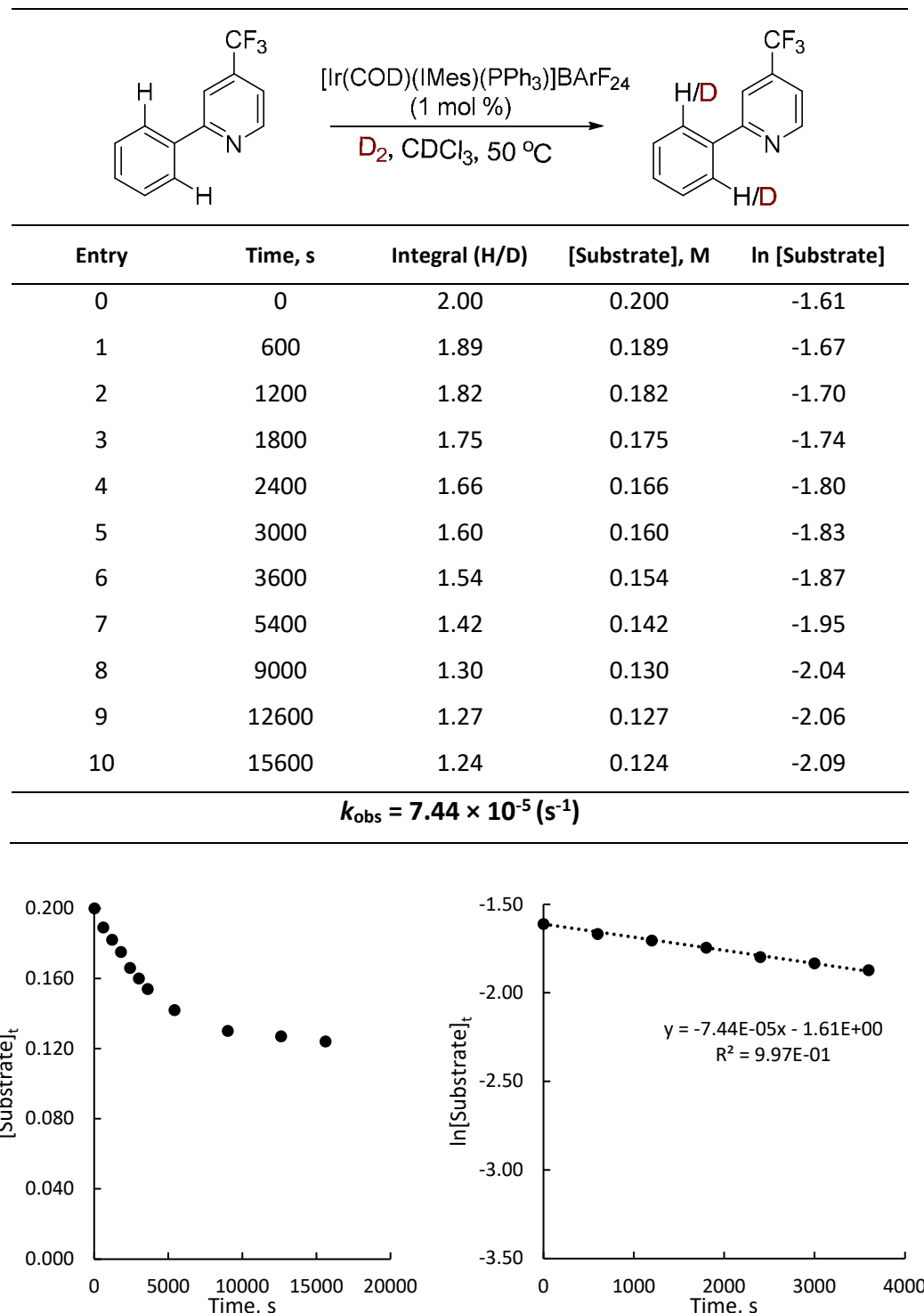


Figure S22. Kinetic profile for the HIE reaction of 4- trifluoromethyl-2-phenyl pyridine over time in CDCl₃ at 50 °C (left). Fitting a first-order kinetic model to the data (right).

Table S24. The extent of deuterium labelling and the distribution of d_0 , d_1 , and d_2 in 4-trifluoromethyl-2-phenyl pyridine as determined by LC-MS analysis (Data from experiment in Table S20).

Observed relative abundances							
		m/z	Ph(H ₂)DG	60 min	120 min	180 min	240 min
(M-H)	d_0	223	100.0	100.0	100.0	71.8	56.0
(M-H)+1	d_1	224	13.3	34.6	63.5	62.0	51.6
(M-H)+2	d_2	225	1.4	38.4	91.1	100.0	100.0
Relative abundances adjusted for natural abundance of isotopes							
		m/z	Ph(H ₂)DG	60 min	120 min	180 min	240 min
(M-H)	d_0	223	100.0	100.0	100.0	71.8	56.0
(M-H)+1	d_1	224	0.0	23.6	50.2	52.4	44.1
(M-H)+2	d_2	225	0.0	32.6	81.6	91.0	92.5
Total abundance			100.0	219.0	187.1	207.4	193.0
Normalised relative abundances							
		m/z	Ph(H ₂)DG	60 min	120 min	180 min	240 min
(M-H)	d_0	223	100.0	64.0	43.2	33.4	29.1
(M-H)+1	d_1	224	0.0	15.1	21.7	24.4	22.9
(M-H)+2	d_2	225	0.0	20.9	35.2	42.3	48.0
Level of deuterium incorporation							
		Ph(H ₂)DG	60 min	120 min	180 min	240 min	
%D by LC-MS		0	28	46	54	59	
%D by NMR		0	33	51	59	63	

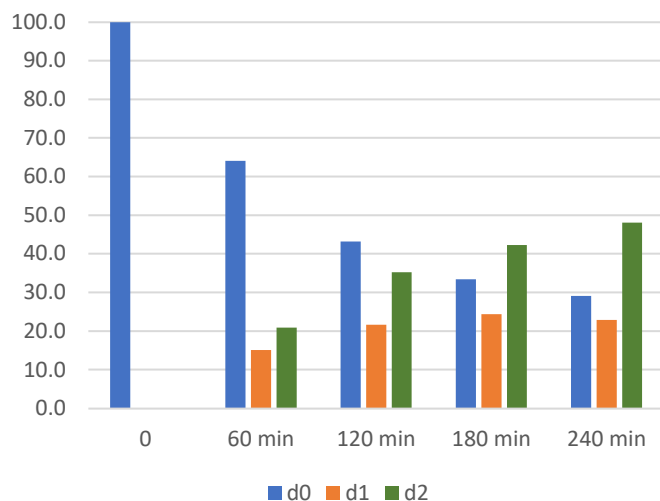
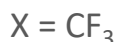
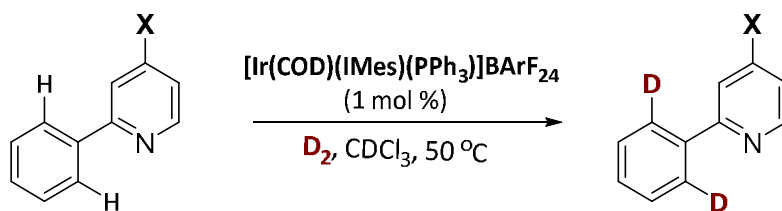


Figure S23. The distribution of d_0 , d_1 , and d_2 during 4-trifluoromethyl-2-phenyl pyridine labelling as determined by LC-MS analysis.

3.4. Hammett plot for substituted phenylpyridines

Table S25. Rate constants for deuteration of 4-substituted 2-Phenylpyridines and Hammett parameters¹³



X	$k_{\text{obs}} (\text{s}^{-1})$	$\log(k_X/k_H)$	σ_p	σ_p^-	σ_p^+
H ^{a,b}	$9.90 \cdot 10^{-5}$	1.00	0.00	0.00	0.00
OMe	$7.96 \cdot 10^{-4}$	0.80	-0.09	-0.27	-0.26
NO ₂	$1.44 \cdot 10^{-4}$	1.45	0.16	0.78	1.27
NH ₂	$6.77 \cdot 10^{-4}$	0.68	-0.17	-0.66	-0.15
CF ₃ (0.38 mmol) ^c	$1.09 \cdot 10^{-4}$	1.10	0.04	0.54	0.65
CF ₃ (0.50 mmol) ^d	$2.00 \cdot 10^{-4}$				
CF ₃ (0.44 mmol)	$1.85 \cdot 10^{-4}$				

^a For X=H k_{obs} from ref.¹⁴; ^b Using 0.50 mmol of substrate; ^c Average of 2 runs; ^d Average of 4 runs;

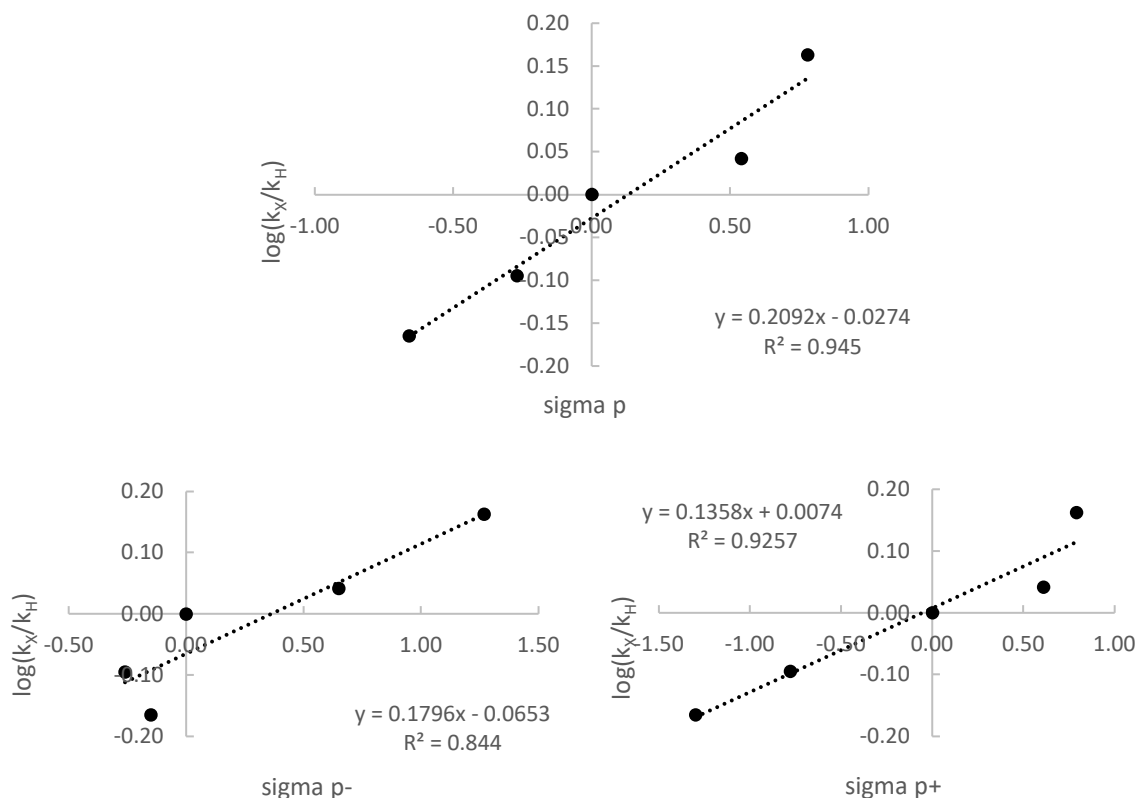


Figure S24. Hammett plots.

4. Computational chemistry

4.1. General computational details

Conformational sampling was conducted using CREST 2.12. DFT calculations were carried out using Gaussian16 Rev C.01.

Geometry optimisations were carried out at 298.15 K without symmetry constraints using the M06-L density functional,¹⁵ the SDD basis set and pseudopotential on iridium,¹⁶ and the 6-311G(d,p) basis set on all other atoms (H, C, N, O, P, Cl). Tight convergence criteria were used for all geometry optimisations. The nature of each stationary point was confirmed using a frequency calculation at 298.15 K. Corrections for temperature (323.15 K), concentration (1 M), and quasiharmonic entropy and enthalpy corrections were applied using GoodVibes.¹⁷

Energies for each species were further refined using single point calculations with the M06-L density functional, the def2-QZVP basis set and – where relevant – associated pseudopotential,^{18,19} and solvation in dichloromethane with the SMD model.²⁰ Free energies quoted in the manuscript are the sum of electronic energy with the larger basis set and the (corrected) correction to free energy obtained with the smaller basis set.

4.2. Energies of optimised structures

Table S26. Energies of optimised structures from DFT calculations: data from optimisation/frequency calculations using a small basis set (6-311G(d,p) + SDD) and data from single point calculations using a large basis set (Def2-QZVP).

Structure	Small Basis: no solvation model			Small Basis: E (Ha)	Large Basis: E (Ha)	
	E (Ha)	G _{corr} (Ha) ^a	G' _{corr} (Ha) ^b	SMD(CHCl ₃)	SMD(DCM)	SMD(CHCl ₃)
<i>Active Catalyst generation</i>						
I-CHCl ₃	-4904.837931	0.638262	0.631475	-4904.916622	N/A	-4905.370873
I-DCM	-3985.660675	0.660029	0.653693	N/A	-3986.163813	N/A
CHCl ₃	-1419.306870	-0.009336	-0.008939	-1419.305408	N/A	-1419.375981
DCM	-959.707643	0.002525	0.003224	N/A	-959.704419	N/A
II-CHCl ₃	-3485.518623	0.622184	0.617418	-3485.605779	N/A	-3485.996414
II-DCM	-3025.927873	0.633406	0.628435	N/A	-3025.299438	N/A
H ₂	-1.171616	-0.001598	0.000504	-1.171312	-1.171112	-1.173323
III-CHCl ₃	-3486.710663	0.641220	0.634990	-3486.789501	N/A	-3487.182681
III-DCM	-3027.118414	0.650688	0.645547	N/A	-3026.472867	N/A
<i>Acetophenone</i>						
Acetophenone	-384.939717	0.104947	0.104647	-384.951760	-385.025002	-385.023803
IV-CHCl ₃	-3870.502685	0.754793	0.747089	-3870.584320	N/A	-3871.04355
IV-DCM	-3410.911774	0.764932	0.757646	N/A	-3411.439640	N/A
V	-2836.161405	0.870853	0.863805	-2836.244017	-2836.714919	-2836.709156
VI	-2451.179789	0.740988	0.735025	-2451.264950	-2451.669379	-2451.662431
TS1	-2451.145441	0.737744	0.731734	-2451.223700	-2451.628984	-2451.622734
VII	-2451.173723	0.740832	0.734768	-2451.252804	-2451.656716	-2451.650798
TS2	-2451.159147	0.739570	0.733538	-2451.250922	-2451.657880	-2451.648661
<i>Nitrobenzene</i>						
Nitrobenzene	-436.813122	0.110568	0.070874	-436.823160	-436.907044	-436.905656
IV-CHCl ₃	-3922.372227	0.717204	0.724324	-3922.452587	N/A	-3922.919509
IV-DCM	-3462.781303	0.883248	0.724324	N/A	-3463.317405	N/A
V	-2939.897824	0.959539	0.792126	-2939.979336	-2940.464924	-2940.45903
VI	-2503.043798	0.846611	0.700180	-2503.128477	-2503.541018	-2503.533724
TS1	-2503.013753	0.842008	0.697512	-2503.092894	-2503.506493	-2503.49985
VII	-2503.044108	0.844631	0.699954	-2503.124129	-2503.536198	-2503.529955
TS2	-2503.025713	0.845584	0.709933	-2503.118009	-2503.533784	-2503.524105
V'	-2503.055534	0.847022	0.709798	-2503.136545	-2503.549155	-2503.542727
<i>Methyl benzoate</i>						
Methyl benzoate	-460.184852	0.152843	0.108205	-460.194731	-460.282036	-460.280917
IV-CHCl ₃	-3945.746696	0.75783	0.762105	-3945.826133	N/A	-3946.299122
IV-DCM	-3486.155314	0.925432	0.762105	N/A	-3486.696089	N/A
V	-2986.638582	1.045223	0.872549	-2986.718065	-2987.215751	-2987.209570
VI	-2526.421835	0.888825	0.736879	-2526.507063	-2526.926889	-2526.918772
TS1	-2526.384460	0.884443	0.735321	-2526.461515	-2526.880582	-2526.874438
VII	-2526.412046	0.887039	0.737749	-2526.490988	-2526.909634	-2526.903533
TS2	-2526.404374	0.888197	0.750658	-2526.489095	-2526.907817	-2526.901682
V'	-2526.409416	0.888804	0.736824	-2526.497802	-2526.918160	-2526.909817
<i>Phenylpyridine</i>						
2-Phenylpyridine	-479.391280	0.178900	0.133908	-479.4061194	-479.495615	-479.494499
IV-CHCl ₃	-3964.955314	0.785897	0.789878	-3965.038861	N/A	-3965.514215
IV-DCM	-3505.362610	0.952322	0.789878	N/A	-3505.909597	N/A
V	-3025.049060	1.097946	0.927240	-3025.138943	-3025.642608	-3025.635146
VI	-2545.643428	0.915604	0.764257	-2545.728144	-2546.149421	-2546.141998

TS1	-2545.610620	0.910923	0.763194	-2545.690872	-2546.112866	-2546.106367
VII	-2545.635606	0.913481	0.765257	-2545.717235	-2546.138818	-2546.132201
TS2	-2545.620256	0.914771	0.776365	-2545.715007	-2546.139086	-2546.129237
<i>2-Methyl-1-phenylimidazole</i>						
2-Methyl-1-phenylimidazole	-496.6393613	0.190362	0.143768	-496.6577431	-496.752600	-496.750617
IV-CHCl₃	-3982.213578	0.794494	0.801045	-3982.296983	N/A	-3982.776283
IV-DCM	-3522.627987	0.963817	0.801045	N/A	-3523.177730	N/A
V	-3059.566448	1.121094	0.948302	-3059.653896	-3060.166837	-3060.158972
VI	-2562.897739	0.927107	0.773557	-2562.984488	-2563.410878	-2563.402672
TS1	-2562.861354	0.922444	0.773032	-2562.941815	-2563.368482	-2563.361587
VII	-2562.885226	0.925084	0.773813	-2562.966773	-2563.392980	-2563.386205
TS2	-2562.884941	0.925735	0.787434	-2562.974647	-2563.401427	-2563.392619
<i>2-Phenylpyrimidine</i>						
2-Phenylpyrimidine	-495.437700	0.166935	0.122193	-495.4529781	-495.544470	-495.5432632
IV-CHCl₃	-3980.997762	0.772933	0.778618	-3981.082321	N/A	-3981.559451
IV-DCM	-3521.408710	0.940058	0.778618	N/A	-3521.956955	N/A
V	-3057.135911	1.073641	0.903153	-3057.227046	-3057.735213	-3057.727359
VI	-2561.686994	0.903703	0.755092	-2561.771724	-2562.194807	-2562.187191
TS1	-2561.652048	0.898926	0.750075	-2561.732636	-2562.156491	-2562.150112
VII	-2561.677985	0.901402	0.753220	-2561.760795	-2562.184577	-2562.177582
TS2	-2561.666008	0.902537	0.764799	-2561.758989	-2562.184516	-2562.175182
<i>1-Phenylpyrazole</i>						
1-Phenylpyrazole	-457.302839	0.160376	0.117215	-457.316402	-457.403509	-457.402148
IV-CHCl₃	-3942.869647	0.770906	0.773915	-3942.951713	N/A	-3943.424039
IV-DCM	-3483.279528	0.933507	0.773915	N/A	-3483.821512	N/A
V	-2980.879903	1.061035	0.894100	-2980.965715	-2981.463099	-2981.455798
VI	-2523.550831	0.896875	0.747240	-2523.637025	-2524.055874	-2524.048000
TS1	-2523.517657	0.892340	0.746302	-2523.598168	-2524.017495	-2524.010835
VII	-2523.544242	0.895024	0.749062	-2523.625711	-2524.044075	-2524.037382
<i>2-Phenylloxazoline</i>						
2-Phenylloxazoline	-478.3958261	0.172188	0.126848	-478.408933	-478.499669	-478.498594
IV-CHCl₃	-3963.968053	0.780856	0.784423	-3964.050133	N/A	-3964.526440
IV-DCM	-3504.378855	0.945505	0.784423	N/A	-3504.923140	N/A
V	-3023.073915	1.085233	0.915155	-3023.158804	-3023.664094	-3023.656852
VI	-2544.650349	0.908962	0.759293	-2544.735137	-2545.157544	-2545.149724
TS1	-2544.610792	0.904482	0.757605	-2544.689647	-2545.111506	-2545.105231
VII	-2544.637886	0.907103	0.759467	-2544.717542	-2545.139605	-2545.133019
TS2	-2544.623980	0.907963	0.772689	-2544.713283	-2545.137226	-2545.128486
<i>For EDA</i>						
VIII	-2066.185739	0.607716	0.604321	N/A	N/A	-2066.609377

a) Uncorrected correction to free energy. b) Correction to free energy after adjusting for temperature (323.15 K), concentration (1 M), and quasiharmonic corrections to entropy and enthalpy.

4.3. Energy decomposition analysis

Structure	M06-L/Def2-QZVP (no solvent model)		
	E (Ha)	E _{dist} (kcal/mol)	E _{int} (kcal/mol)
[Ir(H) ₂ (IMes)(PPh ₃)] (VIII)	-2066.518138		
Acetophenone	-385.011842		
2-Phenylpyridine	-479.480164		
[Ir(H) ₂ (PhAc)(IMes)(PPh ₃)] (VI)			
[Ir(H) ₂ (IMes)(PPh ₃)] fragment	-2066.502547	9.8	--
PhAc fragment	-385.007393	2.8	--
[Ir(H) ₂ (PhAc)(IMes)(PPh ₃)]	-2451.578846	--	-43.2
<i>Total</i>		12.6	-43.2
[Ir(H) ₂ (PhPy)(IMes)(PPh ₃)] (VI)			
[Ir(H) ₂ (IMes)(PPh ₃)] fragment	-2066.499926	11.4	--
PhPy fragment	-479.475577	2.9	--
[Ir(H) ₂ (PhPy)(IMes)(PPh ₃)]	-2546.058870	--	-52.3
<i>Total</i>		14.3	-52.3
[Ir(H) ₂ (PhAc) ₂ (IMes)(PPh ₃)] (V)			
[Ir(H) ₂ (IMes)(PPh ₃)] fragment	-2066.500012	11.4	--
(PhAc) ₂ fragment	-770.015744	5.0	--
[Ir(H) ₂ (PhAc) ₂ (IMes)(PPh ₃)]	-2836.628285	--	-70.6
<i>Total</i>		16.5	-70.6
[Ir(H) ₂ (PhPy) ₂ (IMes)(PPh ₃)] (V)			
[Ir(H) ₂ (IMes)(PPh ₃)] fragment	-2066.487827	19.0	--
(PhPy) ₂ fragment	-958.945172	9.5	--
[Ir(H) ₂ (PhPy) ₂ (IMes)(PPh ₃)]	-3025.546954	--	-71.5
<i>Total</i>		28.5	-71.5
[Ir(H) ₂ (PhAc)(IMes)(PPh ₃)] C-C rotation (TS2)			
[Ir(H) ₂ (IMes)(PPh ₃)] fragment	-2066.503048	9.5	
PhAc fragment	-385.001042	6.8	
TS2	-2451.557894		-33.8
<i>Total</i>		16.3	-33.8
[Ir(H) ₂ (PhPy)(IMes)(PPh ₃)] C-C rotation (TS2)			
[Ir(H) ₂ (IMes)(PPh ₃)] fragment	-2066.491260	16.9	
PhPy fragment	-479.470263	6.2	
TS2	-2546.035321		-46.3
<i>Total</i>		23.1	-46.3

4.4. IRC Electronic Energy Profiles

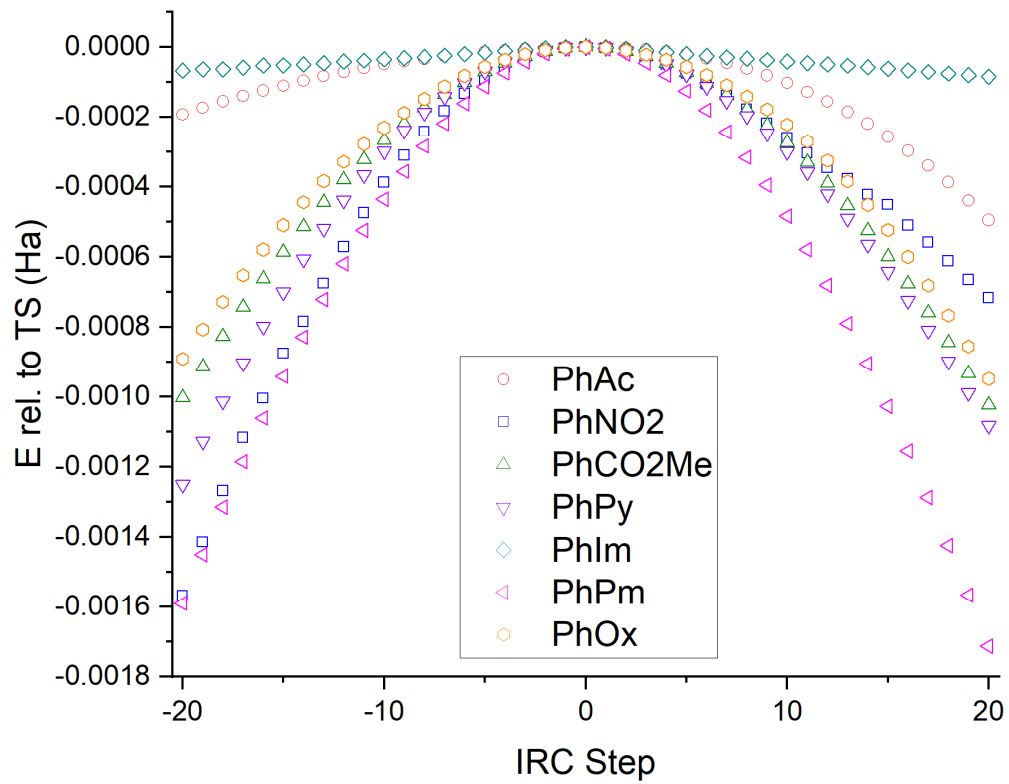


Figure S25. Electronic energy plots for **TS2** for each substrate (except 1-phenylpyrazole, see manuscript text).

4.5. Coordinates of optimised structures

These are supplied as a separate file.

5. Literature Data on Lewis Basicity

Table S27. Lewis basicity quantified using literature data.

Compound	Rel. Directing Ability ²¹ (vs 2-phenylpyridine)	BF ₃ Scale (kJ/mol)	p-FC ₆ H ₄ OH Scale (ΔG°, kJ/mol)	I ₂ Scale (ΔG°, kJ/mol, heptane)	K ⁺ Affinity (298 K, kJ/mol)
Parent					
N-Heterocycles					
1-methyl-imidazole	n/a		-15.53 ²²		117.7 ± 2.7 ²³
Pyridine	n/a	128.08 ± 0.50 ²⁴	-10.62 ²⁵	-12.67 ²⁶	90.6 ± 3.9 ²⁷
1-methyl-pyrazole	n/a		-10.50 ²²	-12.22 ²⁸	94.8 ± 3.6 ²³
Pyrazole	n/a			-10.79 ²⁹	
Pyrimidine	n/a	113.02 ± 0.21 ³⁰	-6.11 ²⁵	-5.59 ³¹	69.7 ± 4.3 ²⁷
N-Heterocyclic Substrates					
2-phenyl-pyridine	1.00		-8.16 ²⁵		
1-phenyl-pyrazole	1.77			-5.71 ²⁸	
Other Substrates					
Acetophenone	0.06	74.52 ± 0.15 ³²			
Ethyl benzoate	0.01	61.2 ± 0.8 ³²			
Nitrobenzene	0.03	35.79 ± 1.40 ²⁴			

6. References.

- 1 A. Beillard, X. Bantreil, T.-X. Métro, J. Martinez and F. Lamaty, *Dalton Trans.*, 2016, **45**, 17859–17866.
- 2 M. R. Kumar, K. Park and S. Lee, *Advanced Synthesis & Catalysis*, 2010, **352**, 3255–3266.
- 3 M. M. Debdab Florence; Bazureau, Jean Pierre, *Synthesis*, 2006, **2006**, 4046–4052.
- 4 J. Yang, S. Liu, J.-F. Zheng and J. (Steve) Zhou, *European Journal of Organic Chemistry*, 2012, **2012**, 6248–6259.
- 5 N. A. Yakelis and R. G. Bergman, *Organometallics*, 2005, **24**, 3579–3581.
- 6 A. J. Martínez-Martínez and A. S. Weller, *Dalton Trans.*, 2019, **48**, 3551–3554.
- 7 A. R. Cochrane, S. Irvine, W. J. Kerr, M. Reid, S. Andersson and G. N. Nilsson, *Journal of Labelled Compounds and Radiopharmaceuticals*, 2013, **56**, 451–454.
- 8 A. R. Kennedy, W. J. Kerr, R. Moir and M. Reid, *Org. Biomol. Chem.*, 2014, **12**, 7927–7931.
- 9 H. Andersson, T. Sainte-Luce Banchelin, S. Das, R. Olsson and F. Almqvist, *Chem. Commun.*, 2010, **46**, 3384–3386.
- 10 P. Guo, J. M. Joo, S. Rakshit and D. Sames, *J. Am. Chem. Soc.*, 2011, **133**, 16338–16341.
- 11 J. Wang, S. Wang, G. Wang, J. Zhang and X.-Q. Yu, *Chem. Commun.*, 2012, **48**, 11769–11771.
- 12 K. L. Billingsley, K. W. Anderson and S. L. Buchwald, *Angewandte Chemie International Edition*, 2006, **45**, 3484–3488.
- 13 C. Hansch, A. Leo and R. W. Taft, *Chem. Rev.*, 1991, **91**, 165–195.
- 14 D. S. Timofeeva, D. M. Lindsay, W. J. Kerr and D. J. Nelson, *Catal. Sci. Technol.*, 2021, **11**, 5498–5504.
- 15 Y. Zhao and D. G. Truhlar, *Theoretical Chemistry Accounts*, 2008, **120**, 215–241.
- 16 D. Andrae, U. Häußermann, M. Dolg, H. Stoll and H. Preuß, *Theoretica chimica acta*, 1990, **77**, 123–141.
- 17 G. Luchini, J. Alegre-Requena, I. Funes-Ardoiz and R. Paton, *F1000Research*, DOI:10.12688/f1000research.22758.1.
- 18 F. Weigend and R. Ahlrichs, *Phys. Chem. Chem. Phys.*, 2005, **7**, 3297–3305.
- 19 F. Weigend, *Phys. Chem. Chem. Phys.*, 2006, **8**, 1057–1065.
- 20 A. V. Marenich, C. J. Cramer and D. G. Truhlar, *J. Phys. Chem. B*, 2009, **113**, 6378–6396.
- 21 D. S. Timofeeva, D. M. Lindsay, W. J. Kerr and D. J. Nelson, *Catal. Sci. Technol.*, 2020, **10**, 7249–7255.

- 22 C. Laurence and J. F. Gal, in *Lewis Basicity and Affinity Scales*, John Wiley & Sons, Chichester, United Kingdom, 1st edn., 2009, pp. 111–227.
- 23 H. Huang and M. T. Rodgers, *J. Phys. Chem. A*, 2002, **106**, 4277–4289.
- 24 P.-C. Maria, J.-F. Gal, J. De Franceschi and E. Fargin, *J. Am. Chem. Soc.*, 1987, **109**, 483–492.
- 25 M. Berthelot, C. Laurence, M. Safar and F. Besseau, *J. Chem. Soc., Perkin Trans. 2*, 1998, 283–290.
- 26 C. Laurence and J. F. Gal, in *Lewis Basicity and Affinity Scales*, John Wiley & Sons, Chichester, United Kingdom, 1st edn., 2009, pp. 229–321.
- 27 R. Amunugama and M. T. Rodgers, *International Journal of Mass Spectrometry*, 2000, **195–196**, 439–457.
- 28 M. J. El Ghomari, R. Mokhlisse, C. Laurence, J.-Y. Le Questel and M. Berthelot, *Journal of Physical Organic Chemistry*, 1997, **10**, 669–674.
- 29 J. L. M. Abboud, R. Notario, M. Berthelot, R. M. Claramunt, P. Cabildo, J. Elguero, M. J. El Ghomari, W. Bouab, R. Mokhlisse and G. Guihéneuf, *J. Am. Chem. Soc.*, 1991, **113**, 7489–7493.
- 30 M. Berthelot, J. F. Gal, C. Laurence and P. C. Maria, *J. Chim. Phys. Phys.-Chim. Biol.*, 1984, **81**, 327–331.
- 31 P. A. Clark, T. J. Lerner, S. Hayes and S. G. Fischer, *J. Phys. Chem.*, 1976, **80**, 1809–1811.
- 32 P. C. Maria and J. F. Gal, *J. Phys. Chem.*, 1985, **89**, 1296–1304.